AIMS Mathematics, 11(2): 4299–4334.
DOI:10.3934/math.2026173
Received: 20 November 2025
Revised: 23 January 2026
Accepted: 03 February 2026
Published: 12 February 2026

https://www.aimspress.com/journal/Math

Research article

Helices with F-constant vector fields in the Euclidean space $\mathbb{E}^4$

Derya Sağlam[1], **Umut Selvi**[1,*], **Faik Babadağ**[2] **and Ali Atasoy**[3]

[1] Department of Mathematics, Ankara Hacı Bayram Veli University, Ankara, 06900, Turkey
[2] Department of Mathematics, Kırıkkale University, Kırıkkale, 71450, Turkey
[3] Keskin Vocational School, Kırıkkale University, Kırıkkale, 71800, Turkey

* **Correspondence:** Email: umut.selvi@hbv.edu.tr; Tel: +903125461425.

Abstract: This study aims to investigate the geometric properties of V_i-helices in the four-dimensional Euclidean space $\mathbb{E}^4$, considering Frenet vector fields as instances of F-constant vector fields. For each $i \in \{1, 2, 3, 4\}$, the necessary and sufficient conditions for V_i-helices are derived in terms of their curvatures, and a generalization of these helices is presented. Examples of these structures are provided, and their projections onto three-dimensional (3D) spaces are visualized using Python. Furthermore, the corresponding Python codes are included in the Appendix.

Keywords: V_i-helix; Darboux vector field; F-constant vector field; Frenet-Serret vector field; cylinder
Mathematics Subject Classification: 53A04, 53A07

1. Introduction

Curves in Euclidean spaces are of great interest in classical differential geometry because of their wide range of applications in both theoretical and applied fields. Among these curves, helices and their generalizations have garnered the most attention owing to their beautiful geometric properties and applications in physics, biology, etc.

A classical helix is defined as a curve whose tangent vector forms a constant angle with a fixed direction in $\mathbb{E}^3$. The concept of generalized helices was developed by extending this idea to a higher-dimensional Euclidean space. The tangent vector field $\gamma(s)$ in $\mathbb{E}^n$ of a curve is referred to as a generalized helix if it creates a fixed unit vector in the space that forms a constant angle. Menninger [1] introduced the successor transformation of Frenet curves and examined helices with successor curves in $\mathbb{E}^3$. Şenol et al. [2] provided new necessary and sufficient characterizations for inclined curves, V_n-slant helices, and V_2-slant helices in $\mathbb{E}^n$ by restructuring the existing conditions and using harmonic curvature functions and other differentiable functions. Ali [3] determined the parametric representation

of position vectors for spacelike general helices in $\mathbb{E}_1^3$ by constructing a third-order vector differential equation and utilizing intrinsic equations, specifically for cases with spacelike and timelike principal normal vectors. Ali and López [4] characterized cylindrical helices in $\mathbb{E}^n$. Camcı et al. [5] examined the characterizations of generalized helices in $\mathbb{E}^4$ using different curvature requirements, extending the earlier work by Özdamar and Hacısalihoğlu, who established the necessary conditions for a curve in $\mathbb{E}^4$ to qualify as a generalized helix. Sağlam [6] provided characterizations of dual slant helices in $\mathbb{D}^3$, exploring their relationship with dual general helices and demonstrating that their dual tangent and binormal indicatrices are dual spherical helices. Ziplar and Şenol [7] characterized Darboux helices in $\mathbb{E}^3$, establishing their coincidence with slant helices and demonstrating that the curves of constant precession are a specific type of Darboux helix when the magnitude of its Darboux vector $|\mathcal{D}| = \sqrt{\tau^2 + \kappa^2}$ is constant. Hayden [8] established that generalized helices in a Riemannian n-space possess a constant angle property with respect to a parallel vector field. Gök et al. [9] introduced and defined V_n-slant helices in $\mathbb{E}^n$ using new harmonic curvature functions and a Darboux vector field $\mathcal{D}$. Barros [10] extended Lancret's theorem for general helices to three-dimensional (3D) real-space-forms, revealing a significant difference between hyperbolic (where no nontrivial general helices exist) and spherical geometries. Barros et al. [11] introduced Lancret-type theorems for general helices in 3D Lorentzian space forms, demonstrating that these curves are geodesics on specific geometric structures. Kula and Yaylı [12] investigated spherical pictures of a slant helix's tangent and binormal indicatrix and found that the spherical pictures are actually spherical helices. Lucas and Ortega-Yagües [13] demonstrated that slant helices are precisely the geodesics of helix surfaces, which are characterized as the tangent surfaces of general helices, and provided two methods for constructing them. They also expanded the notion of a helix in $\mathbb{E}^3$ (see [14]). Öztürk and Alkan [15] presented and described Darboux helices in a Lie group and demonstrated their association with slant and general helices. They also showed that if the group is commutative, then not all Darboux helices are slant helices. Yang [16] presented methods for approximating helix segments using quintic polynomials and rational Bézier curves. Ünlütürk et al. [17] examined k-type pseudo-null slant helices using the Bishop frame in $\mathbb{E}_1^3$, determined the axes and causal characters of these helices for two distinct Bishop frame cases, and demonstrated that all pseudo-null curves are k-type pseudo-null curves.

The geometric product is noncommutative, associative, and distributive upon addition in Euclidean n-space. Let u and v be vectors in $\mathbb{E}^n$ and let $\{e_1, e_2\}$ be an orthonormal basis of the plane formed by the vectors. The geometric product uv of vectors $u = ae_1 + be_2$ and $v = ce_1 + de_2$ is the scalar plus the bivector

$$uv = (ac + bd) + (ad - bc)e_1e_2 = u.v + u \wedge v.$$

The geometric product is an invertible bilinear operation that is the sum of the inner (dot) and outer (wedge) products. The inner and outer products are the symmetric and antisymmetric parts of the geometric product and are as follows, respectively:

$$u.v = \frac{1}{2}(uv + vu), \quad u \wedge v = \frac{1}{2}(uv - vu).$$

For a multivector A, let $(A)_i$ denote its i-vector part. For the multivector uv, we have

$$(uv)_0 = u.v, \quad (uv)_1 = 0, \quad (uv)_2 = u \wedge v.$$

The inner product of the i-vector A and j-vector B is defined as

$$A.B = (AB)_{|j-i|}.$$

Some examples for the orthonormal vectors e_1, e_2, and e_3 are as follows:

$$e_1.(e_1e_2e_3) = (e_1e_1e_2e_3)_{|3-1|} = e_2e_3,$$

$$(e_2e_3).(e_1e_2e_3) = (e_2e_3e_1e_2e_3)_{|3-2|} = -e_1,$$

$$e_2.(e_2e_3) = (e_2e_2e_3)_{|2-1|} = e_3,$$

$$e_1.(e_2e_3) = (e_1e_2e_3)_{|2-1|} = 0, \text{ (see [18])}.$$

Let $\chi(I)$ represent the collection of smooth vector fields along the unit-speed curve $\gamma : I \to \mathbb{E}^3$. A moving orthonormal frame along γ can be represented as $F = \{V_1, V_2, V_3\}$. This allows us to consider F as a differentiable map $F : I \to SO(3)$. There is a unique vector field $\mathcal{D}_\gamma$ along γ that satisfies the equation

$$V_i' = \mathcal{D}_\gamma \times V_i\ ,\quad i \in \{1, 2, 3\}, \tag{1.1}$$

where $\times$ represents the cross-product. This can be easily demonstrated. The Darboux vector associated with the frame F is denoted by $\mathcal{D}_\gamma$. Let us take the well-known Frenet-Serret equations

$$V_1' = \kappa V_2, \quad V_2' = -\kappa V_1 + \tau V_3, \quad V_3' = -\tau V_2, \tag{1.2}$$

where κ, τ, and $F = \{V_1, V_2, V_3\}$ are the curvature function, the torsion function, and a specific moving Frenet frame, respectively. The Darboux vector for this frame is simply $\mathcal{D}_\gamma$, and its value is

$$\mathcal{D}_\gamma = \tau V_1 + \kappa V_3. \tag{1.3}$$

The angular velocity of the complete Frenet frame can be computed using this vector. The frame $\{V_1, V_2, V_3\}$ changes at a rate of s, which may be described as an instantaneous rotation about the vector $\mathcal{D}_\gamma$ with an angular velocity equal to the total curvature given by

$$|\mathcal{D}_\gamma| = \sqrt{\kappa^2 + \tau^2}. \tag{1.4}$$

In Euclidean 3-space, the F-constant vector field is defined as a vector field W along γ if $W' = \mathcal{D}_\gamma \times W$. Thus, it is clear that the Frenet vector fields V_1, V_2, and V_3 are F-constant vector fields (see [14]).

Let $F = \{V_1, V_2, V_3, V_4\}$ be the Frenet frame of a curve γ in the Euclidean 4-space. Similarly, the Frenet vector fields V_1, V_2, V_3, and V_4 of a curve γ are also F-constant vector fields. In the Euclidean 4-space, there is a unique bivector field $\mathcal{D}_\gamma$ along γ that satisfies the equations

$$V_i' = \mathcal{D}_\gamma.V_i\ ,\quad i \in \{1, 2, 3, 4\}, \tag{1.5}$$

where "." represents the inner product of the bivector $\mathcal{D}_\gamma$ and the vector V_i. This can be easily demonstrated. The Darboux bivector associated with the frame F is denoted by $\mathcal{D}_\gamma$. It is worth noting that while the derivative of a vector field in $\mathbb{E}^3$ is conventionally expressed using the cross-product with the Darboux vector, in $\mathbb{E}^4$, this relationship is generalized through the inner product with the Darboux bivector $\mathcal{D}_\gamma$ to account for the higher-dimensional geometry. Let us take the well-known Frenet-Serret equations

$$V_1' = \kappa_1 V_2, \quad V_2' = -\kappa_1 V_1 + \kappa_2 V_3, \quad V_3' = -\kappa_2 V_2 + \kappa_3 V_4, \quad V_4' = -\kappa_3 V_3, \tag{1.6}$$

where κ_1, κ_2, and κ_3 are the curvature functions, and the Frenet frame $F = \{V_1, V_2, V_3, V_4\}$ is a specific moving frame [19]. The Darboux bivector for this frame is simply $\mathcal{D}_\gamma$, and its value is

$$\mathcal{D}_\gamma = \sum_{i=1}^{3} \mathcal{D}_i, \tag{1.7}$$

where $\mathcal{D}_1 = \kappa_1 V_2 \wedge V_1$, $\mathcal{D}_2 = \kappa_2 V_3 \wedge V_2$, and $\mathcal{D}_3 = \kappa_3 V_4 \wedge V_3$. Here, the symbol $\wedge$ denotes an outer product. The angular velocity of the complete Frenet frame can be computed using this bivector. The frame $\{V_1, V_2, V_3, V_4\}$ changes with respect to the arc-length parameter s, which may be described as an instantaneous rotation about the bivector $\mathcal{D}_\gamma$ with an angular velocity equal to the total curvatures given by

$$\|\mathcal{D}_\gamma\| = \sqrt{\sum_{i=1}^{3} \kappa_i^2}, \tag{1.8}$$

where κ_i is the curvature for $i \in \{1, 2, 3\}$ (see more details in [20]). In Euclidean 4-space, a vector field W along γ is called an F-constant vector field if $W' = \mathcal{D}_\gamma.W$. Thus, it is clear that the Frenet vector fields V_1, V_2, V_3, and V_4 are F-constant vector fields.

Along the curve $\gamma : I \to \mathbb{E}^4$, a nonzero differentiable vector field W is considered. When $W(s)$ is a member of the plane orthogonal to V_i for each s, the vector field is considered to be a V_i-vector field for each $i \in \{1, 2, 3, 4\}$. A curve γ is regarded as a helix if an F-constant vector field W exists along γ, creating a constant angle with a fixed direction V, which is the axis of the helix. The curve γ is called a V_i-helix if W is a V_i-vector field. In this paper, we investigate the geometric properties of V_i-helices in the four-dimensional (4D) Euclidean space $\mathbb{E}^4$, considering the Frenet vector fields as instances of F-constant vector fields. For each $i \in \{1, 2, 3, 4\}$, we derive the necessary and sufficient conditions for V_i-helices in terms of their curvatures and present a generalization of these helices. Furthermore, we construct a geometric interpretation of V_1-helices and their relation to cylindrical structures. An illustrative example of this structure is also presented, and its projections onto 3D spaces are visualized using Python.

Throughout this work, the notation $C_{i,j} = \frac{\kappa_i}{\kappa_j}$ will be used for $1 \leq i \neq j \leq 3$.

2. V_1-helices

2.1. Equations of V_1-helices

Suppose that there are nonzero constant angles $\varrho, \xi \in \left(-\frac{\pi}{2}, \frac{\pi}{2}\right)$ such that the unit vector field W, given by

$$W = \sin\varrho \cos\xi V_2 + \sin\varrho \sin\xi V_3 + \cos\varrho V_4, \tag{2.1}$$

is expressed in spherical coordinates within the subspace spanned by $\{V_2, V_3, V_4\}$. In this representation, V_4 serves as the polar axis; consequently, ϱ corresponds to the polar angle (colatitude), while ξ denotes the azimuthal angle measured from the principal normal vector V_2. The constancy of ϱ and ξ implies that W maintains a fixed geometric orientation relative to the Frenet frame. Furthermore, we assume that W is orthogonal to the vector field defined by

$$V = \lambda V_1 + \mu \left(\cos\varrho \cos\xi V_2 + \cos\varrho \sin\xi V_3 - \sin\varrho V_4\right), \tag{2.2}$$

where λ and μ are differentiable functions. After calculating the derivative in (2.2), we have

$$\lambda' - \mu\kappa_1 \cos\varrho \cos\xi = 0, \tag{2.3}$$

$$\lambda\kappa_1 + \mu' \cos\varrho \cos\xi - \mu\kappa_2 \cos\varrho \sin\xi = 0, \tag{2.4}$$

$$\mu' \cos\varrho \sin\xi + \mu\kappa_2 \cos\varrho \cos\xi + \mu\kappa_3 \sin\varrho = 0, \tag{2.5}$$

$$-\mu' \sin\varrho + \mu\kappa_3 \cos\varrho \sin\xi = 0, \tag{2.6}$$

where κ_1, κ_2, and κ_3 are the curvature functions.

From (2.5) and (2.6), we have

$$\frac{\mu'}{\mu} = -\frac{\kappa_2 \cos\varrho \cos\xi + \kappa_3 \sin\varrho}{\cos\varrho \sin\xi}, \tag{2.7}$$

and

$$\frac{\mu'}{\mu} = \frac{\kappa_3 \cos\varrho \sin\xi}{\sin\varrho}. \tag{2.8}$$

From (2.7) and (2.8), we then have

$$\frac{\kappa_3}{\kappa_2} = -\frac{\sin\varrho \cos\varrho \cos\xi}{\sin^2\varrho + \cos^2\varrho \sin^2\xi}. \tag{2.9}$$

From (2.8),

$$\mu = e^{\cot\varrho \sin\xi \int \kappa_3 dt}, \quad \text{and} \quad \mu' = e^{\cot\varrho \sin\xi \int \kappa_3 dt} \kappa_3 \cot\varrho \sin\xi, \tag{2.10}$$

which, when combined with (2.4), results in

$$\lambda = e^{\cot\varrho \sin\xi \int \kappa_3 dt} \cos\varrho \sin\xi \left(\frac{\kappa_2}{\kappa_1} - \frac{\kappa_3}{\kappa_1} \cot\varrho \cos\xi\right), \tag{2.11}$$

as well as this

$$\lambda' = e^{\cot\varrho \sin\xi \int \kappa_3 dt} \cos\varrho \sin\xi \left[\kappa_3 \cot\varrho \sin\xi \left(\frac{\kappa_2}{\kappa_1} - \frac{\kappa_3}{\kappa_1} \cot\varrho \cos\xi\right) + \left(\frac{\kappa_2}{\kappa_1}\right)' - \left(\frac{\kappa_3}{\kappa_1}\right)' \cot\varrho \cos\xi\right]. \tag{2.12}$$

Substituting (2.10), and (2.12) into Eq (2.3), we obtain the following by direct calculation:

$$\sin\xi \left[\kappa_3 \cot\varrho \sin\xi \left(\frac{\kappa_2}{\kappa_1} - \frac{\kappa_3}{\kappa_1} \cot\varrho \cos\xi\right) + \left(\frac{\kappa_2}{\kappa_1}\right)' - \left(\frac{\kappa_3}{\kappa_1}\right)' \cot\varrho \cos\xi\right] = \kappa_1 \cos\xi. \tag{2.13}$$

Multiplying both sides by κ_1 and rearranging the terms involving $\cos\xi$ and $\sin\xi$, we obtain the following relation:

$$\frac{\kappa_1^2 + \cot\varrho \sin\xi(\kappa_3^2 \cot\varrho \sin\xi + C'_{3,1}\kappa_1)}{\kappa_2\kappa_3 \cot\varrho \sin\xi + C'_{2,1}\kappa_1} = \tan\xi, \tag{2.14}$$

where we use the notation $C'_{i,j} = (\kappa_i/\kappa_j)'$.

Theorem 2.1. *Let γ be a unit-speed curve with nonzero curvatures κ_1, κ_2, and κ_3 in $\mathbb{E}^4$. With W orthogonal to V, γ is a V_1-helix if and only if (iff) the following conditions are satisfied:*

$$C_{3,2} = -\frac{\sin\varrho \cos\varrho \cos\xi}{\sin^2\varrho + \cos^2\varrho \sin^2\xi}, \quad \textit{and} \quad \frac{\kappa_1^2 + \cot\varrho \sin\xi(\kappa_3^2 \cot\varrho \sin\xi + C'_{3,1}\kappa_1)}{\kappa_2\kappa_3 \cot\varrho \sin\xi + C'_{2,1}\kappa_1} = \tan\xi. \tag{2.15}$$

Example 2.1. Let $c > 0$ be a real constant. We define the curvature functions $\kappa_1, \kappa_2, \kappa_3$ of a unit-speed curve $\gamma : I \to \mathbb{E}^4$ and the constant angles ϱ, ξ as

$$\kappa_1(s) = c, \quad \kappa_2(s) = \frac{3c}{2}\tan\left(\frac{cs}{2}\right), \quad \kappa_3(s) = -\frac{\sqrt{2}c}{2}\tan\left(\frac{cs}{2}\right), \quad \varrho = \frac{\pi}{4}, \quad \xi = \frac{\pi}{4}. \tag{2.16}$$

Note that the chosen domain I avoids the singularities of the tangent function at $s = \pm\pi/c$. In this context, because κ_1 is constant while κ_2 and κ_3 are nonconstant functions of the arc-length parameter s, the curve is classified as a Salkowski-type curve. Formally, a Salkowski-type curve in $\mathbb{E}^4$ is defined as a curve with a constant first curvature κ_1, whereas its second and third curvatures, κ_2 and κ_3, are nonconstant [21]. These curves are significant in differential geometry because they serve as a primary example of generalized helices in higher-dimensional spaces, where the tangent vector maintains a constant angle in a fixed direction. We now analytically verify that the parameters given in (2.16) satisfy the two conditions of Theorem 2.1.

Condition 1: The curvature ratio. The first condition requires that $C_{3,2} = \frac{\kappa_3}{\kappa_2}$ satisfies:

$$\frac{\kappa_3}{\kappa_2} = -\frac{\sin\varrho\cos\varrho\cos\xi}{\sin^2\varrho + \cos^2\varrho\sin^2\xi}. \tag{2.17}$$

Substituting $\varrho = \xi = \pi/4$ for the right-hand side (RHS) of (2.17), where $\sin(\pi/4) = \cos(\pi/4) = \frac{\sqrt{2}}{2}$, we have

$$\text{RHS} = -\frac{\sqrt{2}}{3}.$$

The ratio of the defined curvatures for the left-hand side (LHS) of (2.17) was verified as follows:

$$\frac{\kappa_3(s)}{\kappa_2(s)} = -\frac{\sqrt{2}}{3}.$$

Because LHS = RHS, the first condition is satisfied.

Condition 2: The differential equation. The second condition is expressed as follows:

$$\frac{\kappa_1^2 + A(A\kappa_3^2 + C'_{3,1}\kappa_1)}{A\kappa_2\kappa_3 + C'_{2,1}\kappa_1} = \tan\xi,$$

where $A = \cot\varrho\sin\xi$. For $\pi/4$, we have $A = 1 \cdot \frac{\sqrt{2}}{2} = \frac{\sqrt{2}}{2}$ and $\tan\xi = 1$. Since $\kappa_1 = c$ is constant, $\kappa_1' = 0$, implying $C'_{i,1}\kappa_1 = \kappa_i'$. The equation is simplified as follows:

$$\kappa_1^2 + A^2\kappa_3^2 + A\kappa_3' = A\kappa_2\kappa_3 + \kappa_2'.$$

Substituting $A = \frac{\sqrt{2}}{2}$, we have

$$c^2 + \frac{1}{2}\kappa_3^2 + \frac{\sqrt{2}}{2}\kappa_3' = \frac{\sqrt{2}}{2}\kappa_2\kappa_3 + \kappa_2'.$$

Using $\kappa_3 = -\frac{\sqrt{2}}{3}\kappa_2$, we can simplify further. It can be shown that this reduces to checking the following identity:

$$\kappa_1^2 + \frac{4}{9}\kappa_2^2 = \frac{4}{3}\kappa_2'.$$

We test this identity using the following functions:

$$\text{LHS} = c^2 \sec^2\left(\frac{cs}{2}\right), \qquad \text{RHS} = c^2 \sec^2\left(\frac{cs}{2}\right).$$

Because LHS = RHS, the second condition is strictly satisfied.

Because the analytical integration of the Frenet equations for this curve involves complex Fresnel-like integrals, we used numerical integration to visualize the curve. The curve is 4D; therefore, we present its projections onto the *xyz*, *xyw*, *xzw*, and *yzw* hyperplanes. Figure 1 shows the numerical results. The *yzw* projection (Figure 1d) clearly exhibits a helical structure arising from the variable curvatures κ_2 and κ_3, which are characteristic of the Salkowski curves. The Python code used to generate these figures is provided in Appendix 1.

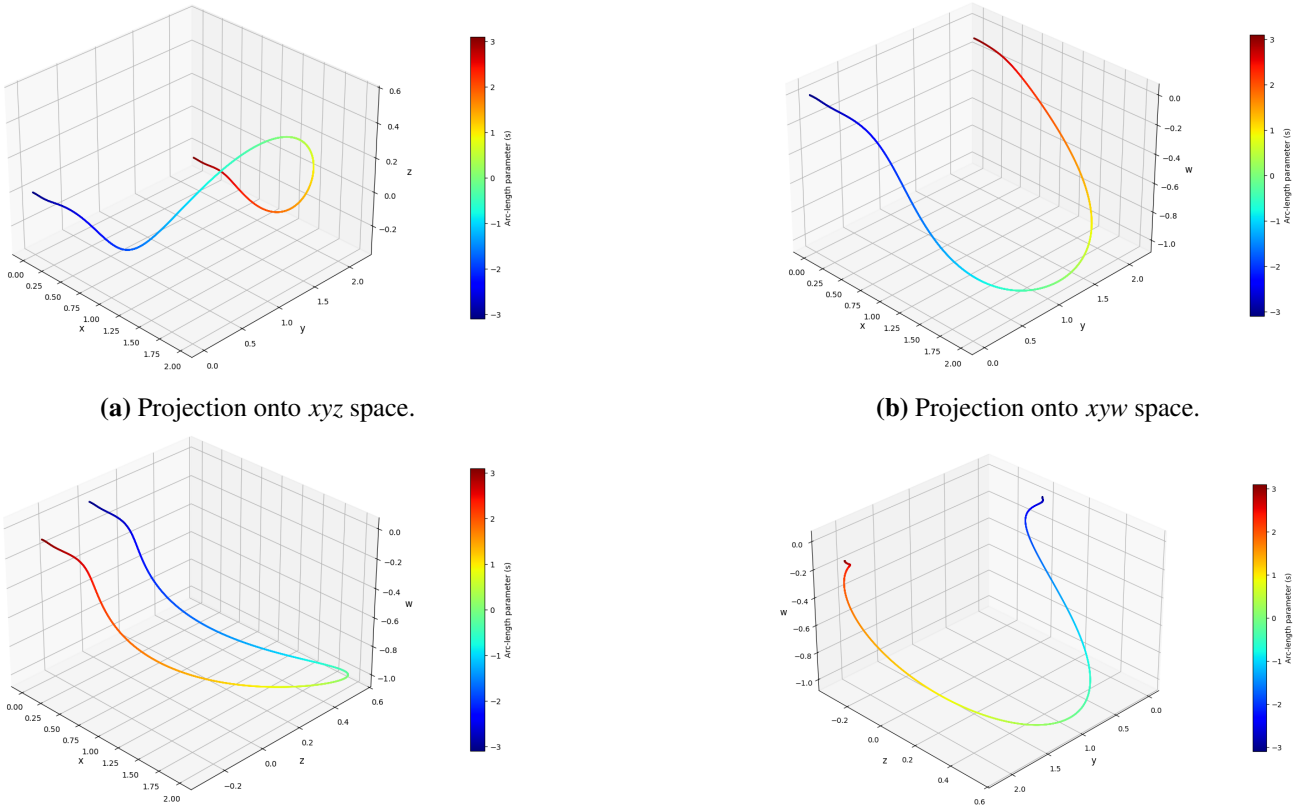

(a) Projection onto *xyz* space.

(b) Projection onto *xyw* space.

(c) Projection onto *xzw* space.

(d) Projection onto *yzw* space.

Figure 1. Projections of the 4D Salkowski-type curve into 3D subspaces. The color indicates the arc-length parameter *s*.

2.2. *Geometric interpretation of* V_1*-helices*

Consider a general cylinder $M = G_{\alpha,V}$ parametrized by $\Theta(t,u) = \alpha(t) + uV$, where α is a unit space curve and V is a unit vector orthogonal to the space. Let $\{T_\alpha, N_\alpha, B_\alpha\}$ be the Frenet frame of α, and let Z_1, Z_2 be the unit normal vectors to the cylinder M. T_α and V span the tangent space of M. Let Z_1 and Z_2 be parallel to N_α and B_α, respectively. Let $Z_1 = N_\alpha$ and $Z_2 = B_\alpha$. Assume further that $\gamma(s) = \Theta(t(s), u(s))$, $s \in I$, is a unit curve in M. The Frenet frame of it is

$$V_1(s) \quad = \quad \cos\delta(s) T_\alpha(t(s)) + \sin\delta(s) V; \tag{2.18}$$

$$V_2(s) = \cos\varrho\cos\xi(-\sin\delta(s)T_\alpha(t(s)) + \cos\delta(s)V) + \sin\varrho\cos\xi Z_1 + \sin\xi Z_2; \tag{2.19}$$

$$V_3(s) = \cos\varrho\sin\xi(-\sin\delta(s)T_\alpha(t(s)) + \cos\delta(s)V) + \sin\varrho\sin\xi Z_1 - \cos\xi Z_2; \tag{2.20}$$

$$V_4(s) = -\sin\varrho(-\sin\delta(s)T_\alpha(t(s)) + \cos\delta(s)V) + \cos\varrho Z_1, \tag{2.21}$$

where the function δ is differentiable with

$$t'(s) = \cos\delta(s), \quad \text{and} \quad u'(s) = \sin\delta(s). \tag{2.22}$$

It is clear that,

$$V = \sin\delta(s)V_1 + \cos\varrho\cos\delta(s)[\cos\xi V_2 + \sin\xi V_3] - \sin\varrho\cos\delta(s)V_4. \tag{2.23}$$

The F-constant vector field $W = \sin\varrho\cos\xi V_2 + \sin\varrho\sin\xi V_3 + \cos\varrho V_4$ may then be defined, fulfilling $\langle W, V\rangle = 0$ and demonstrating that γ is a V_1-helix. Thus, we demonstrated the following outcomes.

Theorem 2.2. *A V_1-helix with an axis V is a curve γ in $\mathbb{E}^4$ iff γ lies on a cylinder M and its Frenet vector fields V_3 and V_4 form constant angles with the cylinder's normal vector fields Z_2 and Z_1, respectively.*

By taking the derivatives (2.18), (2.19), and (2.21), we have

$$\kappa_1(s)V_2(s) = -\delta'(s)\sin\delta(s)T_\alpha(t(s)) + \kappa_\alpha(t(s))\cos\delta(s)N_\alpha(t(s))t'(s) + \delta'(s)\cos\delta(s)V; \tag{2.24}$$

$$\begin{aligned} -\kappa_1(s)V_1(s)+\kappa_2(s)V_3(s) &= \cos\varrho\cos\xi(-\delta'(s)\cos\delta(s)T_\alpha(t(s))-\kappa_\alpha(t(s))\sin\delta(s)\cos\delta(s)N_\alpha(t(s)) \\ -\delta'(s)\sin\delta(s)V)+\sin\varrho\cos\xi\cos\delta(s)(-\kappa_\alpha(t(s))T_\alpha(t(s))+\tau_\alpha(t(s))B_\alpha(t(s))-\tau_\alpha(t(s))\sin\xi N_\alpha(t(s))), \end{aligned} \tag{2.25}$$

and

$$\begin{aligned} \kappa_3(s)V_3(s) = &-\sin\varrho[\delta'(s)\cos\delta(s)T_\alpha(t(s)) + \kappa_\alpha(t(s))\sin\delta(s)\cos\delta(s)N_\alpha(t(s)) + \delta'(s)\sin\delta(s)V] \\ &-\cos\varrho\cos\delta(s)[-\kappa_\alpha(t(s))T_\alpha(t(s)) + \tau_\alpha(t(s))B_\alpha(t(s))]. \end{aligned} \tag{2.26}$$

From Eqs (2.24)–(2.26), we obtain the following theorem.

Theorem 2.3. *Let $\gamma(s) = \Theta(t(s), u(s))$ be a unit-speed curve in the general cylinder $M = G_{\alpha,V}$. Its Frenet vector fields V_3 and V_4 form a constant angle with the cylinder's normal vector fields Z_2 and Z_1, respectively, iff there is a differentiable function δ such that the following equations are satisfied:*

$$t'(s) = \cos\delta(s); \tag{2.27}$$

$$u'(s) = \sin\delta(s); \tag{2.28}$$

$$\delta'(s) = \kappa_\alpha(t(s))\cos^2\delta(s)\cot\varrho. \tag{2.29}$$

In addition, the curvatures of the curve γ are obtained as follows:

$$\kappa_1(s) = \kappa_\alpha(t(s))\cos^2\delta(s)\csc\varrho\sec\xi; \tag{2.30}$$

$$\kappa_2(s) = -\cos\delta(s)(\kappa_\alpha(t(s))\cot\varrho\cot\xi\sin\delta(s) + \tau_\alpha(t(s))\csc\varrho); \tag{2.31}$$

$$\kappa_3(s) = -\kappa_\alpha(t(s))\sin\delta(s)\cos\delta(s)\csc\xi. \tag{2.32}$$

Moreover, multiplying both sides of Eqs (2.20) and (2.26) by $N_\alpha(t(s))$ and $B_\alpha(t(s))$, we have

$$\kappa_\alpha(t(s)) = \kappa_1(s)\sec^2\delta(s)\sin\varrho\cos\xi, \tag{2.33}$$

and

$$\tau_\alpha(t(s)) = -\kappa_\alpha(t(s))\sin\delta(s)\sec\varrho\cot\xi, \tag{2.34}$$

respectively. Since $(\tan\delta(s))' = \delta'(s)\sec^2\delta(s)$, we have

$$(\tan\delta(s))' = \kappa_\alpha(t(s))\cot\varrho. \tag{2.35}$$

Remark 2.1. *It is important to emphasize the geometric distinction between the V_1-helix and subsequent types. As seen in Eq (2.18), the tangent vector V_1 resides entirely within the tangent space of the cylinder M, spanned by T_α and V. This intrinsic property allows the V_1-helix to be characterized as a curve with a constant slope on the cylinder. Conversely, the vector fields V_2, V_3, and V_4 (Eqs (2.19) and (2.20)) contain nonzero components along the cylinder's normal vectors Z_1 and Z_2. Therefore, while the V_2-, V_3-, and V_4-helices are defined by their orthogonality to the fixed axis V, their interaction with the supporting cylinder is extrinsic, governed by the orientation of the frame's normal components rather than the tangent trajectory alone.*

Example 2.2. Let $\Theta(t,u) = \alpha(t) + uV$ where $\alpha(t) = (\cos t, \sin t, 0, 0)$ and $V = (0,0,1,1)$. Let (x,y,z,w) be the Cartesian coordinate system of $\mathbb{E}^4$. The following curve is a V_1-helix:

$$\gamma(s) = \Theta(t(s), u(s)) = (\cos t(s), \sin t(s), u(s), u(s)),$$

where $t(s) = \tan\varrho\sinh^{-1}(s\cot\varrho) + t_0$ and $u(s) = \tan\varrho\sqrt{1+(s\cot\varrho)^2} + u_0$. From (2.29), we have

$$\delta(s) = \arctan(s\cot\varrho). \tag{2.36}$$

For simplicity, we set the integration constants to zero. From (2.36), we get

$$\cos\delta(s) = \frac{\sin\varrho}{\sqrt{\sin^2\varrho + s^2\cos^2\varrho}},$$

and

$$\sin\delta(s) = \frac{s\cos\varrho}{\sqrt{\sin^2\varrho + s^2\cos^2\varrho}}.$$

In addition, because $\kappa_\alpha = 1$ and $\tau_\alpha = 0$, from (2.30)–(2.32), we find the curvature of the curve γ in the following equations:

$$\begin{aligned}
\kappa_1(s) &= \frac{\sin\varrho\sec\xi}{\sin^2\varrho + s^2\cos^2\varrho},\\
\kappa_2(s) &= -\frac{s\cos^2\varrho\cot\xi}{\sin^2\varrho + s^2\cos^2\varrho},\\
\kappa_3(s) &= -\frac{s\sin\varrho\cos\varrho\csc\xi}{\sin^2\varrho + s^2\cos^2\varrho}.
\end{aligned}$$

Indeed, changing the parameters $s\cot\varrho = \sinh(t\cot\varrho)$, we have

$$\gamma(t) = (\cos(t+t_0), \sin(t+t_0), \omega(t), \omega(t)),$$

where $\omega(t) = \tan\varrho\cosh(t\cot\varrho) + u_0$ and its curvatures are

$$\begin{aligned}
\kappa_1(s) &= \frac{\csc\varrho\sec\xi}{\cosh^2(t\cot\varrho)},\\
\kappa_2(s) &= -\frac{\sinh(t\cot\varrho)\cot\varrho\cot\xi}{\cosh^2(t\cot\varrho)},\\
\kappa_3(s) &= -\frac{\sinh(t\cot\varrho)\csc\xi}{\cosh^2(t\cot\varrho)}.
\end{aligned}$$

The projection of the 4D curve $\gamma(t)$ onto the 3D subspaces (xyz, xyw, xzw, yzw) is displayed in Figure 2.

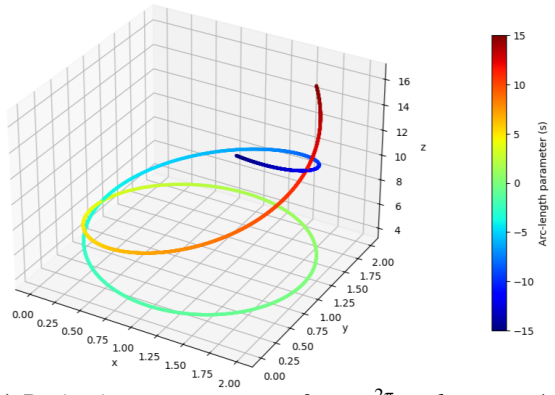

(a) *Projection onto xyz space for* $\varrho = \frac{2\pi}{5}$ *and* $t_0 = u_0 = 1$.

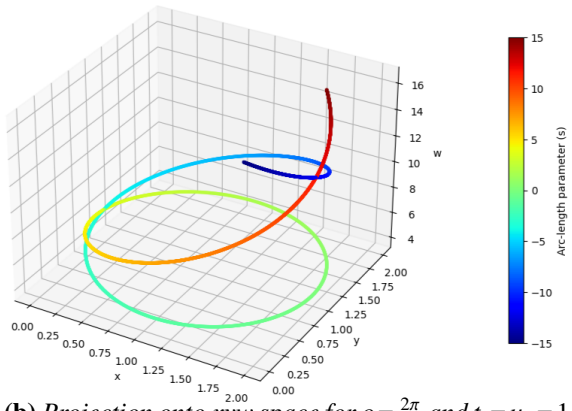

(b) *Projection onto xyw space for* $\varrho = \frac{2\pi}{5}$ *and* $t_0 = u_0 = 1$.

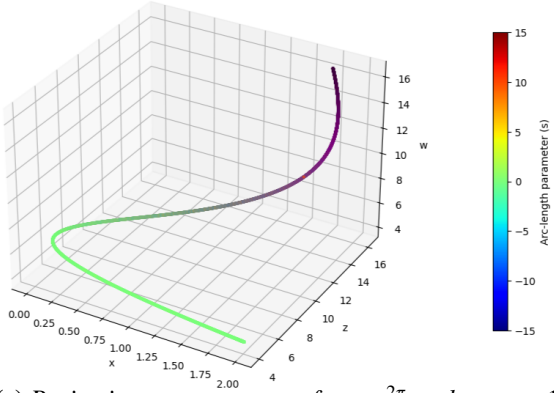

(c) *Projection onto xzw space for* $\varrho = \frac{2\pi}{5}$ *and* $t_0 = u_0 = 1$.

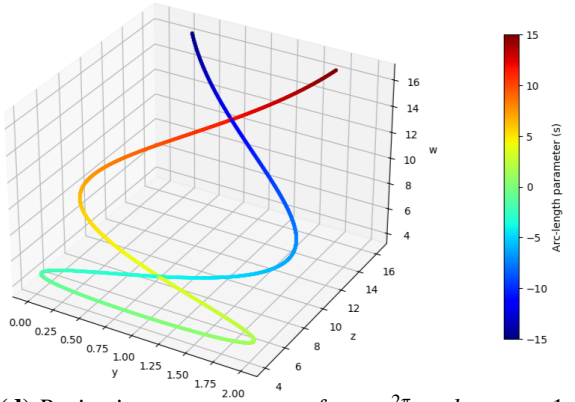

(d) *Projection onto yzw space for* $\varrho = \frac{2\pi}{5}$ *and* $t_0 = u_0 = 1$.

Figure 2. Projections of the geometric interpretation of a V_1-helix. The color indicates the arc-length parameter s.

3. V_2-helices

Suppose that there are nonzero constant angles $\varrho, \xi \in \left(-\frac{\pi}{2}, \frac{\pi}{2}\right)$ such that the unit vector field W, given by

$$W = \sin\varrho\cos\xi V_1 + \sin\varrho\sin\xi V_3 + \cos\varrho V_4, \tag{3.1}$$

is expressed in spherical coordinates within the subspace spanned by $\{V_1, V_3, V_4\}$. In this representation, V_4 serves as the polar axis; consequently, ϱ corresponds to the polar angle (colatitude), while ξ denotes the azimuthal angle measured from the tangent vector V_1. The constancy of ϱ and ξ implies that W maintains a fixed geometric orientation relative to the Frenet frame. Furthermore, we assume that W is orthogonal to the vector field defined by

$$V = \lambda V_2 + \mu\left(\cos\varrho\cos\xi V_1 + \cos\varrho\sin\xi V_3 - \sin\varrho V_4\right), \tag{3.2}$$

where λ and μ are differentiable functions. When we take the derivative in (3.2), we have

$$-\lambda\kappa_1 + \mu'\cos\varrho\cos\xi = 0; \tag{3.3}$$

$$\lambda' + \mu\cos\varrho(\kappa_1\cos\xi - \kappa_2\sin\xi) = 0; \tag{3.4}$$

$$\lambda\kappa_2 + \mu'\cos\varrho\sin\xi + \mu\kappa_3\sin\varrho = 0; \tag{3.5}$$

$$-\mu'\sin\varrho + \mu\kappa_3\cos\varrho\sin\xi = 0, \tag{3.6}$$

where κ_1, κ_2, and κ_3 are the curvature functions.

From (3.6), we have

$$\mu = e^{\cot\varrho\sin\xi\int\kappa_3 dt}, \quad \text{and} \quad \mu' = e^{\cot\varrho\sin\xi\int\kappa_3 dt}\kappa_3\cot\varrho\sin\xi. \tag{3.7}$$

From (3.3), we have

$$\lambda = \frac{\mu'\cos\varrho\cos\xi}{\kappa_1}. \tag{3.8}$$

Substituting (3.7) and (3.8) into Eq (3.5), we have

$$\frac{\mu'}{\mu} = -\frac{\kappa_1\kappa_3 tan\varrho}{\kappa_1\sin\xi + \kappa_2\cos\xi}. \tag{3.9}$$

Combining (3.7) and (3.9), we have

$$C_{2,1} = -\frac{\tan^2\varrho + \sin^2\xi}{\cos\xi\sin\xi}. \tag{3.10}$$

By entering the equations above into the formula (3.4), we have

$$\cot\varrho\sin\xi\left(\cot\varrho\sin\xi C_{3,2}C_{3,1} + \frac{C'_{3,1}}{\kappa_2}\right) + C_{1,2} = \tan\xi. \tag{3.11}$$

Theorem 3.1. *Let γ be a unit-speed curve with the nonzero curvatures κ_1, κ_2, and κ_3 in $\mathbb{E}^4$. With W orthogonal to V, γ is a V_2-helix iff the following conditions are satisfied:*

$$C_{2,1} = -\frac{\tan^2\varrho + \sin^2\xi}{\cos\xi\sin\xi} \quad \textit{and} \quad \cot\varrho\sin\xi\left(\cot\varrho\sin\xi C_{3,2}C_{3,1} + \frac{C'_{3,1}}{\kappa_2}\right) + C_{1,2} = \tan\xi. \tag{3.12}$$

Example 3.1. Let us define the curvature functions κ_1, κ_2, and κ_3 of a unit-speed curve $\gamma : I \to \mathbb{E}^4$

$$\kappa_1(s) = 1, \quad \kappa_2(s) = 2, \quad \kappa_3(s) = \sqrt{3}\tan(\sqrt{3}s). \tag{3.13}$$

Note that $\kappa_3(s) = \sqrt{3}\tan(\sqrt{3}s)$ has singularities at $s = \frac{\pi}{2\sqrt{3}}$, so the curve is properly defined only on the open interval $I = (-\frac{\pi}{2\sqrt{3}}, \frac{\pi}{2\sqrt{3}})$. We select the constant angles ϱ and ξ as

$$\varrho = \arcsin\frac{1}{\sqrt{3}}, \quad \xi = -\frac{\pi}{4}. \tag{3.14}$$

We now verify that these choices satisfy Theorem 3.1. From (3.14), we have

$$\sin\varrho = \frac{1}{\sqrt{3}}, \quad \cos\varrho = \frac{\sqrt{2}}{\sqrt{3}}, \quad \tan\varrho = \frac{1}{\sqrt{2}}, \quad \cot\varrho = \sqrt{2};$$
$$\sin\xi = -\frac{1}{\sqrt{2}}, \quad \cos\xi = \frac{1}{\sqrt{2}}, \quad \tan\xi = -1.$$

Condition 1: The curvature ratio. The first criterion requires $C_{2,1} = -\frac{\tan^2\varrho+\sin^2\xi}{\cos\xi\sin\xi}$.

$$\begin{aligned} \text{LHS} &= C_{2,1} = \frac{\kappa_2}{\kappa_1} = \frac{2}{1} = 2, \\ \text{RHS} &= -\frac{(\frac{1}{\sqrt{2}})^2 + (-\frac{1}{\sqrt{2}})^2}{(\frac{1}{\sqrt{2}})(-\frac{1}{\sqrt{2}})} = -\frac{\frac{1}{2}+\frac{1}{2}}{-\frac{1}{2}} = -\frac{1}{-\frac{1}{2}} = 2. \end{aligned}$$

Since LHS = RHS, the condition holds.

Condition 2: The differential equation. The second criterion is the following differential equation:

$$\cot\varrho\sin\xi\left(\cot\varrho\sin\xi C_{3,2}C_{3,1} + \frac{C'_{3,1}}{\kappa_2}\right) + C_{1,2} = \tan\xi.$$

Let $\cot\varrho\sin\xi = \sqrt{2}\cdot(-\frac{1}{\sqrt{2}}) = -1$. Using (3.13), the ratios are

$$C_{3,1} = \sqrt{3}\tan(\sqrt{3}s), \quad C_{3,2} = \frac{\sqrt{3}}{2}\tan(\sqrt{3}s), \quad C_{1,2} = \frac{1}{2}.$$

The derivative is $C'_{3,1} = 3(1+\tan^2(\sqrt{3}s))$. Substituting these values in (3.12), we have

$$\begin{aligned} &\cot\varrho\sin\xi\left(\cot\varrho\sin\xi C_{3,2}C_{3,1} + \frac{C'_{3,1}}{\kappa_2}\right) + C_{1,2} \\ =&(-1)\left[\frac{\sqrt{3}}{2}\tan(\sqrt{3}s)\cdot\sqrt{3}\tan(\sqrt{3}s)\right] + \frac{3(1+\tan^2(\sqrt{3}s))}{2} = -\frac{3}{2}\tan^2(\sqrt{3}s) + \frac{3}{2} + \frac{3}{2}\tan^2(\sqrt{3}s) = \frac{3}{2}. \end{aligned}$$

Finally, substituting back into the main equation, we have

$$(-1)\left(\frac{3}{2}\right) + C_{1,2} = (-1)\left(\frac{3}{2}\right) + \frac{1}{2} = -\frac{3}{2} + \frac{1}{2} = -1.$$

Because $\tan \xi = -1$, the equation $-1 = -1$ is perfectly satisfied.

The coordinate functions of the curve were obtained by numerically integrating the Frenet equations. In Figure 3, the results were visualized by projecting the 4D curve onto 3D subspaces (xyz, xyw, xzw, yzw). The Python code used to generate these figures is provided in Appendix 2.

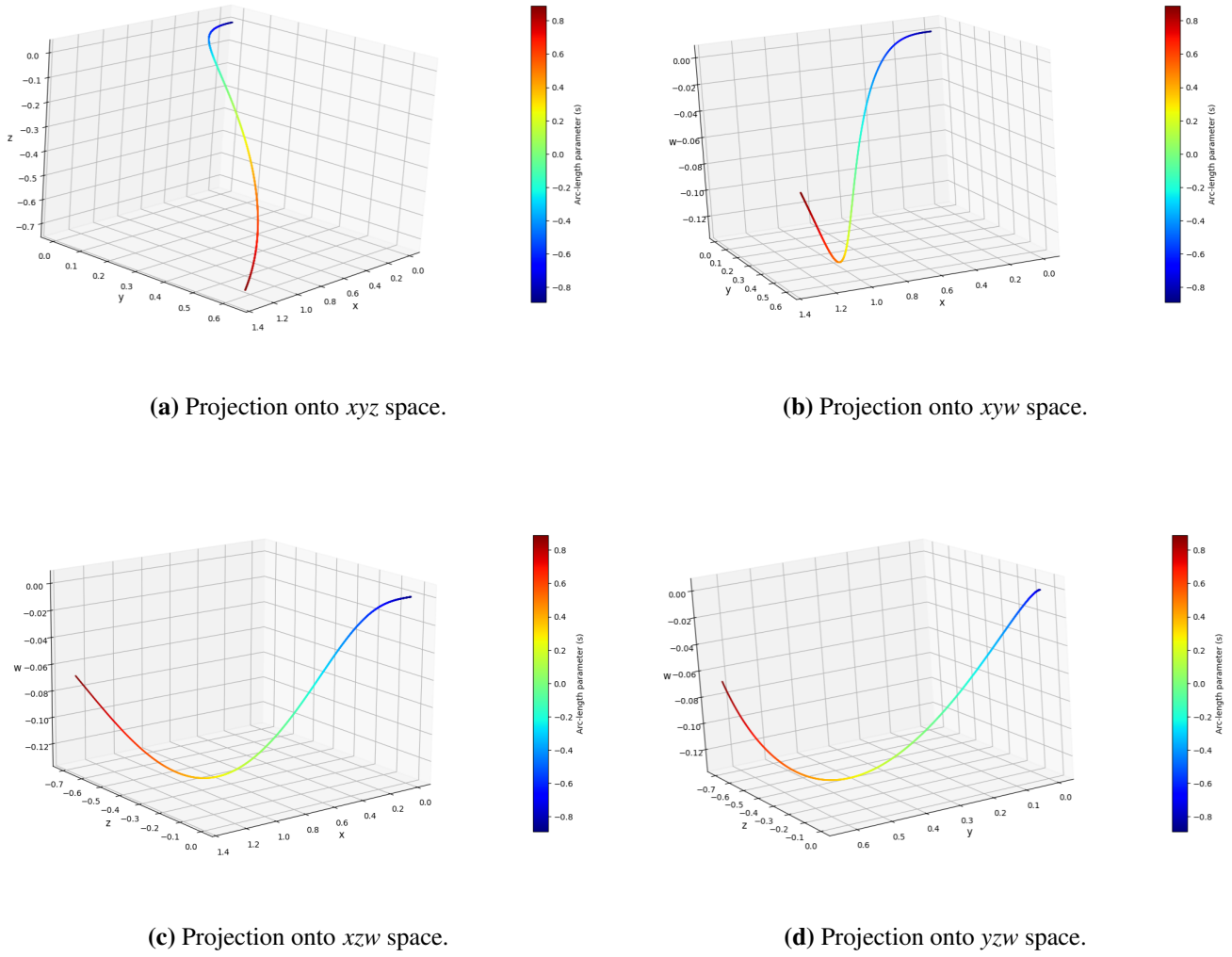

(a) Projection onto xyz space.

(b) Projection onto xyw space.

(c) Projection onto xzw space.

(d) Projection onto yzw space.

Figure 3. Projections of the V_2-helix. The color indicates the arc-length parameter s. The expansion in w-projections corresponds to the singularity of $\tan(\sqrt{3}s)$.

4. V_3-helices

Suppose that there are nonzero constant angles $\varrho, \xi \in \left(-\frac{\pi}{2}, \frac{\pi}{2}\right)$ such that the unit vector field W, given by

$$W = \sin\varrho\cos\xi V_1 + \sin\varrho\sin\xi V_2 + \cos\varrho V_4, \tag{4.1}$$

is expressed in spherical coordinates within the subspace spanned by $\{V_1, V_2, V_4\}$. In this representation, V_4 serves as the polar axis; consequently, ϱ corresponds to the polar angle (colatitude), while ξ denotes

the azimuthal angle measured from the tangent vector V_1. The constancy of ϱ and ξ implies that W maintains a fixed geometric orientation relative to the Frenet frame. Furthermore, we assume that W is orthogonal to the vector field defined by

$$V = \lambda V_3 + \mu\left(\cos\varrho\cos\xi V_1 + \cos\varrho\sin\xi V_2 - \sin\varrho V_4\right), \tag{4.2}$$

where λ and μ are differentiable functions. By taking the derivative in (4.2), we have

$$\mu'\cos\varrho\cos\xi - \mu\kappa_1\cos\varrho\sin\xi = 0; \tag{4.3}$$

$$-\lambda\kappa_2 + \mu'\cos\varrho\sin\xi + \mu\kappa_1\cos\varrho\cos\xi = 0; \tag{4.4}$$

$$\lambda' + \mu(\kappa_2\cos\varrho\sin\xi + \kappa_3\sin\varrho) = 0; \tag{4.5}$$

$$\lambda\kappa_3 - \mu'\sin\varrho = 0, \tag{4.6}$$

where κ_1, κ_2, and κ_3 are curvature functions.

From (4.3), we have

$$\mu = e^{\tan\xi\int\kappa_1 dt} \quad \text{and} \quad \mu' = e^{\tan\xi\int\kappa_1 dt}\kappa_1\tan\xi. \tag{4.7}$$

From (4.5), we have

$$\lambda' = e^{\tan\xi\int\kappa_1 dt}\sin\varrho\tan\xi\left(\frac{\kappa_1^2}{\kappa_3}\tan\xi + (\frac{\kappa_1}{\kappa_3})'\right). \tag{4.8}$$

From (4.4), we then have

$$\frac{\mu'}{\mu} = \frac{\kappa_1\kappa_3\cos\varrho\cos\xi}{\kappa_2\sin\varrho - \kappa_3\cos\varrho\sin\xi}. \tag{4.9}$$

From (4.7) and (4.9), we have

$$C_{3,2} = \tan\varrho\sin\xi. \tag{4.10}$$

In Eq (4.5), substituting (4.10), we have

$$-C_{1,3}^2 = \frac{\cot\xi}{\kappa_3}C_{1,3}' + \frac{\cot^2\xi}{\sin^2\varrho}. \tag{4.11}$$

Theorem 4.1. *Let γ be a unit-speed curve with the nonzero curvatures κ_1, κ_2, and κ_3 in $\mathbb{E}^4$. With W orthogonal to V, γ is a V_3-helix iff the following conditions are satisfied:*

$$C_{3,2} = \tan\varrho\sin\xi \quad \textit{and} \quad C_{1,3}^2 = -\frac{\cot\xi}{\kappa_3}C_{1,3}' - \frac{\cot^2\xi}{\sin^2\varrho}. \tag{4.12}$$

Example 4.1. Let us define the curvature functions κ_1, κ_2, and κ_3 of a unit-speed curve $\gamma : I \to \mathbb{E}^4$ and the constant angles ϱ, ξ as follows:

$$\kappa_1(s) = -\frac{s}{s^2+2} \quad \kappa_2(s) = -\frac{\sqrt{2}}{s^2+2}, \quad \kappa_3(s) = -\frac{1}{s^2+2}, \tag{4.13}$$

where s is the arc-length parameter. We select the constant angles as follows:

$$\varrho = \frac{\pi}{4}, \quad \text{and} \quad \xi = \frac{\pi}{4}.$$

Consequently, the trigonometric values are $\tan\varrho = 1$, $\sin\varrho = \frac{1}{\sqrt{2}}$, $\cot\xi = 1$, and $\sin\xi = \frac{1}{\sqrt{2}}$. We now verify that these functions satisfy the necessary and sufficient conditions derived for a V_3-helix with a constant axis V

$$C_{3,2} = \tan\varrho \sin\xi \quad \text{and} \quad C_{1,3}^2 = -\frac{\cot\xi}{\kappa_3} C'_{1,3} - \frac{\cot^2\xi}{\sin^2\varrho}. \tag{4.14}$$

Condition 1: The curvature ratio. The ratio $C_{3,2}$ is defined as $\frac{\kappa_3}{\kappa_2}$. Substituting the functions from (4.13), we have

$$C_{3,2} = \frac{1}{\sqrt{2}}.$$

For the RHS, using the selected angles, we have

$$\tan\varrho \sin\xi = \frac{1}{\sqrt{2}}.$$

Because LHS = RHS, the first condition is satisfied.

Condition 2: The differential equation. We first calculate $C_{1,3} = \frac{\kappa_1}{\kappa_3}$ as follows:

$$C_{1,3} = s.$$

It follows that $C'_{1,3} = \frac{d}{ds}(s) = 1$. The LHS of the second condition is

$$\text{LHS} = s^2.$$

We now evaluate the RHS. The constant term is

$$\frac{\cot^2\xi}{\sin^2\varrho} = 2.$$

The term involving the derivative is

$$-\frac{\cot\xi}{\kappa_3} C'_{1,3} = s^2 + 2.$$

Combining these into the full expression, we have

$$\text{RHS} = s^2.$$

Since LHS $= s^2$ and RHS $= s^2$, the second condition is satisfied. Thus, the curve defined by the curvatures in (4.13) is a V_3-helix.

Because the curve defined by (4.13) is transcendental, we used numerical integration for its visualization. The Frenet equations in $\mathbb{E}^4$ were solved using the Runge-Kutta method. The resulting curve is projected onto the four principal 3D subspaces: *xyz*, *xyw*, *xzw*, and *yzw*. As shown in Figure 4, the curve exhibits helical characteristics for various projections. The nontrivial nature of the curve in the fourth dimension is evident from the *xyw*, *xzw*, and *yzw* projections.The Python code used to generate these figures is provided in Appendix 3.

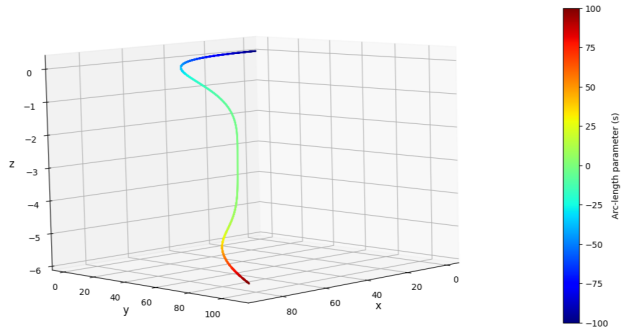

(a) Projection onto xyz space ($w = 0$).

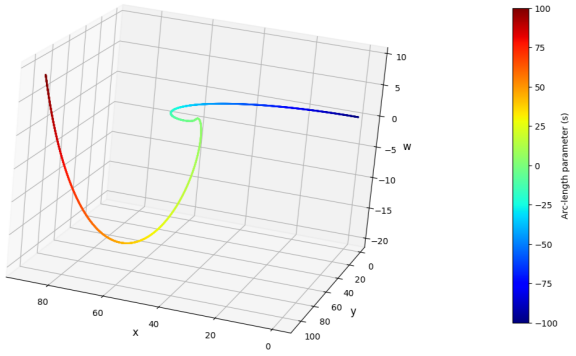

(b) Projection onto xyw space ($z = 0$).

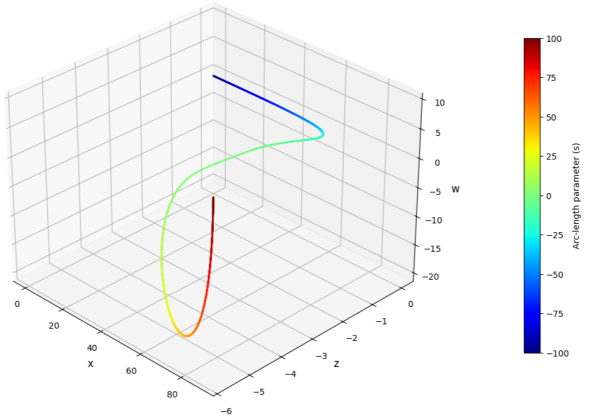

(c) Projection onto xzw space ($y = 0$).

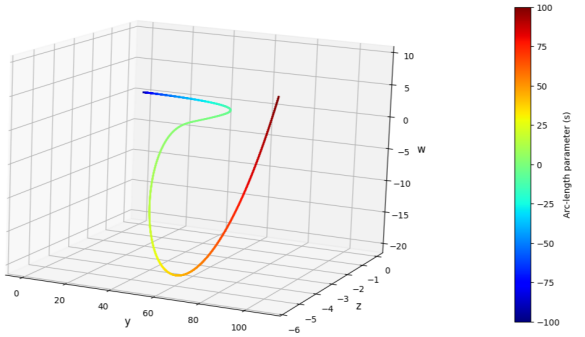

(d) Projection onto yzw space ($x = 0$).

Figure 4. Projections of the V_3-helix into the 3D coordinate subspaces. The color indicates the arc-length parameter s.

5. V_4-helices

Suppose that there are nonzero constant angles $\varrho, \xi \in \left(-\frac{\pi}{2}, \frac{\pi}{2}\right)$ such that the unit vector field W, given by

$$W = \sin\varrho\cos\xi V_1 + \sin\varrho\sin\xi V_2 + \cos\varrho V_3, \tag{5.1}$$

is expressed in spherical coordinates within the subspace spanned by $\{V_1, V_2, V_3\}$. In this representation, V_3 serves as the polar axis; consequently, ϱ corresponds to the polar angle (colatitude), while ξ denotes the azimuthal angle measured from the tangent vector V_1. The constancy of ϱ and ξ implies that W maintains a fixed geometric orientation relative to the Frenet frame. Furthermore, we assume that W is orthogonal to the vector field defined by

$$V = \lambda V_4 + \mu\left(\cos\varrho\cos\xi V_1 + \cos\varrho\sin\xi V_2 - \sin\varrho V_3\right), \tag{5.2}$$

where λ and μ are differentiable functions. After calculating the derivative in (5.2), we have

$$\mu' \cos\varrho \cos\xi - \mu\kappa_1 \cos\varrho \sin\xi = 0; \tag{5.3}$$

$$\mu' \cos\varrho \sin\xi + \mu(\kappa_1 \cos\varrho \cos\xi + \kappa_2 \sin\varrho) = 0; \tag{5.4}$$

$$-\lambda\kappa_3 - \mu' \sin\varrho + \mu\kappa_2 \cos\varrho \sin\xi = 0; \tag{5.5}$$

$$\lambda' - \mu\kappa_3 \sin\varrho = 0, \tag{5.6}$$

where κ_1, κ_2, and κ_3 are the curvature functions.

From (5.3), we have

$$\mu = e^{\tan\xi \int \kappa_1 dt}, \quad \text{and} \quad \mu' = e^{\tan\xi \int \kappa_1 dt} \kappa_1 \tan\xi. \tag{5.7}$$

From (5.4), we have

$$\frac{\mu'}{\mu} = -\frac{\kappa_1 \cos\varrho \cos\xi + \kappa_2 \sin\varrho}{\cos\varrho \sin\xi}. \tag{5.8}$$

From (5.7) and (5.8), we have

$$C_{1,2} = -\tan\varrho \cos\xi. \tag{5.9}$$

Substituting (5.7) into Eq (5.5), we have

$$\lambda' = -\mu' \left(\frac{\kappa_1}{\kappa_3} \sin\varrho \tan\xi - \frac{\kappa_2}{\kappa_3} \cos\varrho \sin\xi\right) - \mu \left(\left(\frac{\kappa_1}{\kappa_3}\right)' \sin\varrho \tan\xi - \left(\frac{\kappa_2}{\kappa_3}\right)' \cos\varrho \sin\xi\right). \tag{5.10}$$

By substituting (5.10) into Eq (5.6), we have

$$\frac{\mu'}{\mu} = -\frac{(\frac{\kappa_1}{\kappa_3})' \sin\varrho \tan\xi - (\frac{\kappa_2}{\kappa_3})' \cos\varrho \sin\xi + \kappa_3 \sin\varrho}{\frac{\kappa_1}{\kappa_3} \sin\varrho \tan\xi - \frac{\kappa_2}{\kappa_3} \cos\varrho \sin\xi}. \tag{5.11}$$

By combining Eqs (5.7), (5.9), and (5.11), we perform a direct calculation to derive the final constraint. First, using the relation $C_{1,3} = -\tan\varrho \cos\xi C_{2,3}$ derived from (5.9), we simplify the denominator D and the numerator N of the RHS of (5.11). Assuming constant angular functions ($\varrho' = \xi' = 0$), we obtain

$$\begin{aligned} D &= \sin\varrho \tan\xi \left(-\frac{\kappa_2}{\kappa_3} \tan\varrho \cos\xi\right) - \frac{\kappa_2}{\kappa_3} \cos\varrho \sin\xi \\ &= -\frac{\sin\xi}{\cos\varrho} C_{2,3} (\sin^2\varrho + \cos^2\varrho) = -\frac{\sin\xi}{\cos\varrho} C_{2,3}. \end{aligned}$$

Similarly, the numerator becomes $N = -\frac{\sin\xi}{\cos\varrho} C'_{2,3} + \kappa_3 \sin\varrho$. Substituting these into (5.11) and equating to $\frac{\mu'}{\mu} = \kappa_1 \tan\xi$ from (5.7), we have

$$\kappa_1 \tan\xi = -\frac{-\frac{\sin\xi}{\cos\varrho} C'_{2,3} + \kappa_3 \sin\varrho}{-\frac{\sin\xi}{\cos\varrho} C_{2,3}} = -\frac{C'_{2,3}}{C_{2,3}} + \frac{\kappa_3 \sin\varrho \cos\varrho}{\sin\xi C_{2,3}}. \tag{5.12}$$

Expressing κ_1 in terms of $C_{2,3}$ as $\kappa_1 = -\kappa_3 \tan\varrho \cos\xi C_{2,3}$, and by rearranging the terms, we obtain

$$\sin\xi \frac{C'_{2,3}}{\kappa_3} - \sin^2\xi \tan\varrho C^2_{2,3} = \sin\varrho \cos\varrho. \tag{5.13}$$

Multiplying by 2 yields the following simplified condition:

$$2\left(\sin\xi \frac{C'_{2,3}}{\kappa_3} - C^2_{2,3} \tan\varrho \sin^2\xi\right) = \sin 2\varrho. \tag{5.14}$$

Theorem 5.1. *Let γ be a unit-speed curve with nonzero curvatures κ_1, κ_2, and κ_3 in $\mathbb{E}^4$. With W orthogonal to V, γ is a V_4-helix iff the following conditions are satisfied:*

$$C_{1,2} = -\tan\varrho\cos\xi \quad \textit{and} \quad 2(\sin\xi\frac{C'_{2,3}}{\kappa_3} - C_{2,3}^2\tan\varrho\sin^2\xi) = \sin 2\varrho. \tag{5.15}$$

Example 5.1. Let $\gamma : I \subset \mathbb{R} \to \mathbb{E}^4$ be a unit-speed curve. We propose the following curvature functions and constant angles:

$$\kappa_1(s) = \frac{-s}{1+s^2}, \quad \kappa_2(s) = \frac{s\sqrt{2}}{1+s^2}, \quad \kappa_3(s) = \frac{\sqrt{2}}{1+s^2}; \tag{5.16}$$

$$\varrho = \frac{\pi}{4}, \quad \xi = \frac{\pi}{4}. \tag{5.17}$$

According to the main theorem, for γ to be a V_4-helix with the vector field V defined in Eq (5.2), two specific criteria must be met. We verify these below.

Condition 1: The curvature ratio. The ratio of the first two curvatures must satisfy:

$$C_{1,2} = -\tan\varrho\cos\xi. \tag{5.18}$$

It is clear that by substituting Eq (5.16) into (5.17), we obtain LHS = RHS.

Condition 2: The differential equation. The differential relationship involving the third curvature must satisfy:

$$2\left(\sin\xi\frac{C'_{2,3}}{\kappa_3} - C_{2,3}^2\tan\varrho\sin^2\xi\right) = \sin 2\varrho. \tag{5.19}$$

By substituting the curvatures and angles, we deduce that (5.19) holds.

Because the analytical integration of the Frenet equations with the curvatures given in (5.16) is nontrivial, we use numerical methods to visualize the curve. We utilize the classical Runge-Kutta method to solve the system of differential equations as follows:

$$\begin{bmatrix} V_1' \\ V_2' \\ V_3' \\ V_4' \end{bmatrix} = \begin{bmatrix} 0 & \kappa_1 & 0 & 0 \\ -\kappa_1 & 0 & \kappa_2 & 0 \\ 0 & -\kappa_2 & 0 & \kappa_3 \\ 0 & 0 & -\kappa_3 & 0 \end{bmatrix} \begin{bmatrix} V_1 \\ V_2 \\ V_3 \\ V_4 \end{bmatrix}. \tag{5.20}$$

The integration was performed over the interval $s \in [-50, 50]$ with the initial conditions corresponding to the standard basis at the origin. The resulting curve is projected onto the four principal 3D subspaces of $\mathbb{E}^4$ (xyz, xyw, xzw, and yzw) in Figure 5. The Python code used to generate these figures is provided in Appendix 4.

Remark 5.1. *It is observed that the first curvature function $\kappa_1(s)$ defined in* (5.16) *takes negative values for $s > 0$. Although the first curvature is traditionally defined as nonnegative in classical Euclidean geometry, we adopted a signed curvature convention in this context. This approach permits the Frenet vector fields to remain smooth and well-defined across the domain, and the sign of κ_1 simply indicates the orientation of the principal normal vector field V_2 relative to the curve's turning direction.*

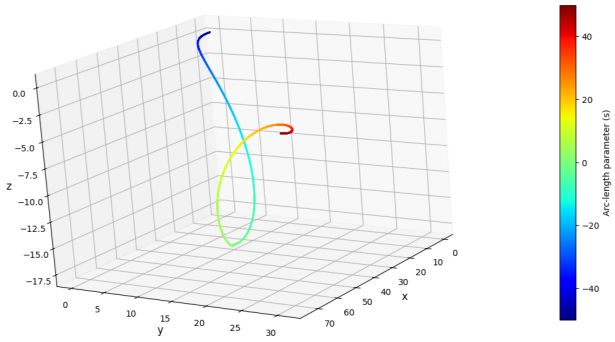

(a) Projection onto xyz space.

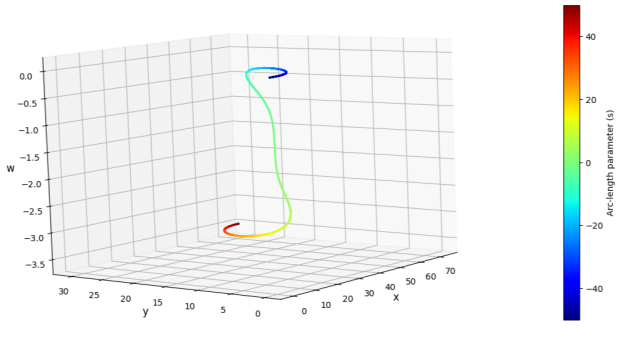

(b) Projection onto xyw space.

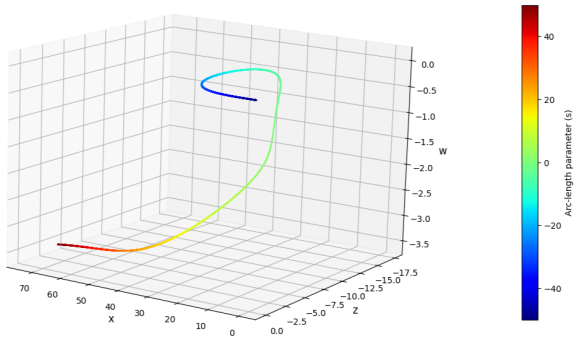

(c) Projection onto xzw space.

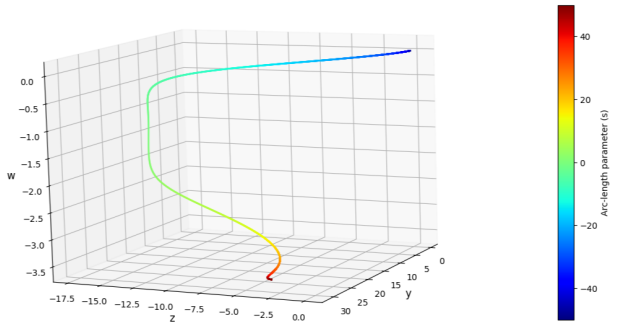

(d) Projection onto yzw space.

Figure 5. Projections of the V_4-helix with variable curvatures. The color indicates the arc-length parameter s. Note the helical structure twisting into the fourth dimension (w-axis) in parts (b), (c), and (d).

6. Helices in the general situation

Suppose that there are constants $a, b, c, d \in \mathbb{R}$ such that $W = aV_1 + bV_2 + cV_3 + dV_4$ is orthogonal to

$$V = \lambda(-cV_1 + dV_2 + aV_3 + -bV_4) + \mu(bV_1 - aV_2 - dV_3 + cV_4), \tag{6.1}$$

where λ, μ are differentiable functions. Taking (6.1) as a derivative gives us

$$-\lambda' c - \lambda d\kappa_1 + \mu' b + \mu a\kappa_1 = 0; \tag{6.2}$$

$$\lambda' d - \lambda(c\kappa_1 + a\kappa_2) - \mu' a + \mu(b\kappa_1 + d\kappa_2) = 0; \tag{6.3}$$

$$\lambda' a + \lambda(d\kappa_2 + b\kappa_3) - \mu' d - \mu(a\kappa_2 + c\kappa_3) = 0; \tag{6.4}$$

$$-\lambda' b + \lambda a\kappa_3 + \mu' c - \mu d\kappa_3 = 0, \tag{6.5}$$

where κ_1, κ_2, and κ_3 are the curvature functions.

From (6.2), we have

$$\lambda' = -\lambda\frac{d}{c}\kappa_1 + \mu'\frac{b}{c} + \mu\frac{a}{c}\kappa_1. \tag{6.6}$$

Substituting (6.6) into Eq (6.5), we have

$$\lambda = \frac{(b^2 - c^2)\mu' + (ab\kappa_1 + cd\kappa_3)\mu}{bd\kappa_1 + ac\kappa_3}. \tag{6.7}$$

By substituting (6.6) and (6.7) into Eq (6.4), we then have

$$\mu' = g\mu, \tag{6.8}$$

where

$$g = \frac{(-ad\kappa_1 + cd\kappa_2 + bc\kappa_3)(ab\kappa_1 + cd\kappa_3) + (bd\kappa_1 + ac\kappa_3)(a^2\kappa_1 - ac\kappa_2 + c^2\kappa_3)}{(-ad\kappa_1 + cd\kappa_2 + bc\kappa_3)(b^2 - c^2) + (bd\kappa_1 + ac\kappa_3)(ab - cd)}.$$

Moreover, substituting (6.6)–(6.8) into (6.3), we have

$$[(ab\kappa_1 + cd\kappa_3) + (c^2 - b^2)g]((c^2 + d^2)\kappa_1 + ac\kappa_2) = [ad + b\kappa_1 + d\kappa_2 + (ac - bd)g](bd\kappa_1 + ac\kappa_3). \tag{6.9}$$

From (6.6)–(6.8), we have

$$\lambda = h\mu \quad \text{and} \quad \lambda' = (h' + hg)\mu, \tag{6.10}$$

where

$$h = \frac{(ab\kappa_1 + cd\kappa_3) + (b^2 - c^2)g}{bd\kappa_1 + ac\kappa_3}.$$

By substituting (6.10) into Eq (6.3), we have

$$d(h' + hg) - (c\kappa_1 + a\kappa_2)h - ag + (b\kappa_1 + d\kappa_2) = 0. \tag{6.11}$$

Theorem 6.1. *Let γ be a unit-speed curve with nonzero curvatures κ_1, κ_2, and κ_3 in $\mathbb{E}^4$. With*

$$W = aV_1 + bV_2 + cV_3 + dV_4$$

orthogonal to

$$V = \lambda(-cV_1 + dV_2 + aV_3 + -bV_4) + \mu(bV_1 - aV_2 - dV_3 + cV_4),$$

γ is a generalized helix iff

$$[(ab\kappa_1 + cd\kappa_3) + (c^2 - b^2)g]((c^2 + d^2)\kappa_1 + ac\kappa_2) = [ad + b\kappa_1 + d\kappa_2 + (ac - bd)g](bd\kappa_1 + ac\kappa_3), \tag{6.12}$$

and

$$d(h' + hg) - (c\kappa_1 + a\kappa_2)h - ag + (b\kappa_1 + d\kappa_2) = 0, \tag{6.13}$$

where

$$g = \frac{(-ad\kappa_1 + cd\kappa_2 + bc\kappa_3)(ab\kappa_1 + cd\kappa_3) + (bd\kappa_1 + ac\kappa_3)(a^2\kappa_1 - ac\kappa_2 + c^2\kappa_3)}{(-ad\kappa_1 + cd\kappa_2 + bc\kappa_3)(b^2 - c^2) + (bd\kappa_1 + ac\kappa_3)(ab - cd)},$$

and

$$h = \frac{(ab\kappa_1 + cd\kappa_3) + (b^2 - c^2)g}{bd\kappa_1 + ac\kappa_3}.$$

We now provide analogs of Theorems 2.2 and 2.3 for the geometric interpretation of helices in a general situation. We assume that $M = G_{\alpha,V}$ is a general cylinder parameterized by $\Theta(t,u) = \alpha(t) + uV$ and that the curve $\gamma(s) = \Theta(t(s),u(s))$ is a unit curve in M. The Frenet frame of the curve γ was given by (2.18)–(2.21). Let these equations and (2.23) be satisfied for the nonconstant functions δ, ϱ, and ξ. Note that $\cos\delta$ is not equal to zero. Otherwise, the curve γ is a planar curve. Similar to Theorem 2.2, the following theorem can then be obtained.

Theorem 6.2. *Let γ be a unit-speed curve with nonzero curvatures κ_1, κ_2, and κ_3 in $\mathbb{E}^4$. In this case, γ is a helix related to the unit F-constant vector field*

$$W = aV_1 + bV_2 + cV_3 + dV_4$$

orthogonal to the axis

$$V = \sin\delta V_1 + \cos\varrho\cos\delta[\cos\xi V_2 + \sin\xi V_3] - \sin\varrho\cos\delta V_4,$$

iff the cylinder $G_{\alpha,V}$ contains γ, which satisfies the following equation:

$$a\tan\delta + \cos\varrho(b\cos\xi + c\sin\xi) - d\sin\varrho = 0, \tag{6.14}$$

where the real variables a, b, c, and d and the angles δ, ϱ, and ξ are related by

$$\begin{aligned}
\langle V_1, V\rangle &= \sin\delta;\\
\langle V_2, V\rangle &= \cos\varrho\cos\delta\cos\xi;\\
\langle V_3, V\rangle &= \cos\varrho\cos\delta\sin\xi;\\
\langle V_4, V\rangle &= -\sin\varrho\cos\delta.
\end{aligned}$$

By differentiating Eq (6.14) and using Eqs (2.27), (2.28), and (2.33)–(2.35), on the basis of Theorem 6.2 and similar to Theorem 2.3, we obtain the following result.

Theorem 6.3. *Let $\gamma(s) = \Theta(t(s),u(s))$ be a unit-speed curve in the general cylinder $M = G_{\alpha,V}$. Then Eq (6.14) holds for the nonconstant functions ϱ and ξ, both of which depend on the variable s, iff*

$$t'(s) = \frac{a}{\sqrt{a^2 + (d\sin\varrho - \cos\varrho(b\cos\xi + c\sin\xi))^2}}, \tag{6.15}$$

$$u'(s) = \frac{d\sin\varrho - \cos\varrho(b\cos\xi + c\sin\xi)}{\sqrt{a^2 + (d\sin\varrho - \cos\varrho(b\cos\xi + c\sin\xi))^2}}, \tag{6.16}$$

$$\kappa_\alpha(t(s)) = \frac{\varrho'(b\sin\varrho\cos\xi + c\sin\varrho\sin\xi + d\cos\varrho) + \xi'(b\cos\varrho\sin\xi - c\cos\varrho\cos\xi)}{a\cot\varrho}, \tag{6.17}$$

$$\begin{aligned}
\tau_\alpha(t(s)) = &-\cot\xi\sec\varrho\frac{d\sin\varrho - \cos\varrho(b\cos\xi + c\sin\xi)}{\sqrt{a^2 + (d\sin\varrho - \cos\varrho(b\cos\xi + c\sin\xi))^2}}\\
&.\frac{\varrho'(b\sin\varrho\cos\xi + c\sin\varrho\sin\xi + d\cos\varrho) + \xi'(b\cos\varrho\sin\xi - c\cos\varrho\cos\xi)}{a\cot\varrho}.
\end{aligned} \tag{6.18}$$

Remark 6.1. *Equations (6.17) and (6.18) establish an intrinsic relationship between the geometry of the generating base curve α and the angular properties of the curve γ on the cylinder. Specifically, Eq*

(6.17) expresses the curvature κ_α of the cross-section solely in terms of the angular functions ϱ and ξ, whereas Eq (6.18) does the same for the torsion τ_α. Geometrically, these equations dictate the precise shape that the base of the cylinder must possess to support a curve γ defined by the given angular variations.

Example 6.1. We present a comprehensive example in which all the deformation parameters of the vector field W are active ($a, b, c, d \neq 0$). Let

$$a = 1, \quad b = 1, \quad c = 1, \quad d = \sqrt{2}, \quad \xi = \frac{\pi}{4},$$

$$\delta(s) = -\arctan(s), \quad \textit{and} \quad \varrho(s) = \frac{\pi}{4} + \arcsin\left(\frac{s}{2}\right), \quad s \in (-2, 2).$$

Substituting the parameters into Eq (6.14), we have

$$a\tan\delta(s) + [d\sin\varrho(s) - \cos\varrho(s)(b\cos\xi + c\sin\xi)] = -s + \left[2\sin\left(\left(\frac{\pi}{4} + \arcsin\frac{s}{2}\right) - \frac{\pi}{4}\right)\right] = 0.$$

Equation (6.14) is satisfied. Substituting the parameters into Theorem 6.3 yields the intrinsic properties of the curve and surface. We then obtain

$$t(s) = \int \frac{ds}{\sqrt{1+s^2}} = \operatorname{arcsinh}(s), \quad u(s) = \int \frac{s\,ds}{\sqrt{1+s^2}} = \sqrt{1+s^2}.$$

With $\xi' = 0$, we have

$$\kappa_\alpha(t(s)) = \tan(\varrho(s)) = \tan\left(\frac{\pi}{4} + \arcsin\frac{s}{2}\right),$$
$$\tau_\alpha(t(s)) = -\sec(\varrho(s))\tan(\varrho(s))\frac{s}{\sqrt{1+s^2}}.$$

Because $\tau_\alpha \neq 0$, the cylinder is generated by a spatial curve (spiral) rather than a planar one. The resulting unit-speed curve $\gamma(s)$ in $\mathbb{E}^4$ is given by

$$\gamma(s) = \alpha(\operatorname{arcsinh} s) + \sqrt{1+s^2}\,\mathbf{e}_4,$$

where α is the curve of the Frenet system determined by the curvature functions $(\kappa_\alpha, \tau_\alpha)$.

The integration was performed over the interval $s \in [-4000, 4000]$ with the initial conditions corresponding to the standard basis at the origin. The resulting curve is projected onto the four principal 3D subspaces of $\mathbb{E}^4$ (*xyz*, *xyw*, *xzw*, and *yzw*) in Figure 6. The Python code used to generate these figures is provided in Appendix 5.

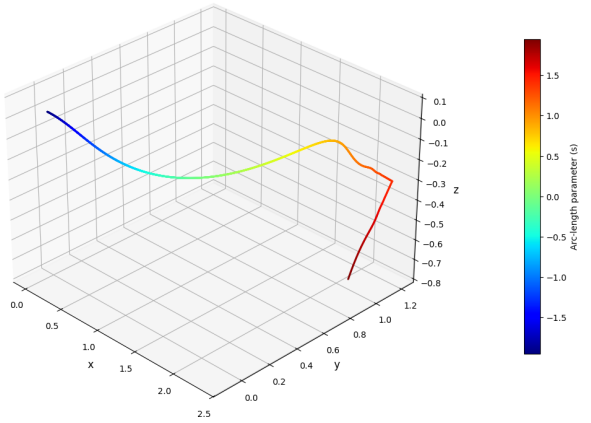

(a) Projection onto xyz space.

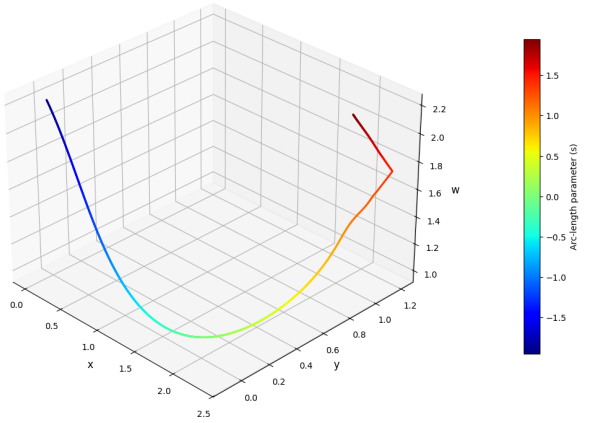

(b) Projection onto xyw space.

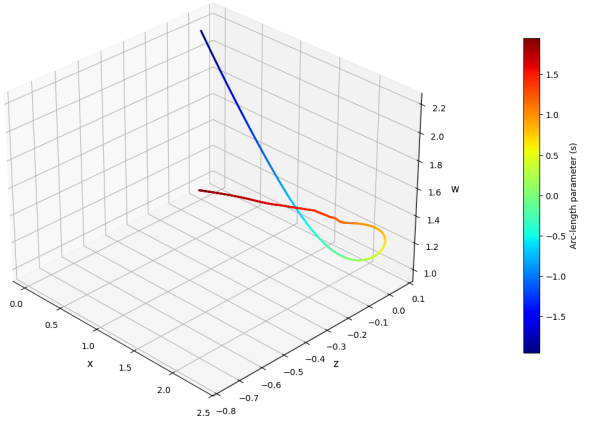

(c) Projection onto xzw space.

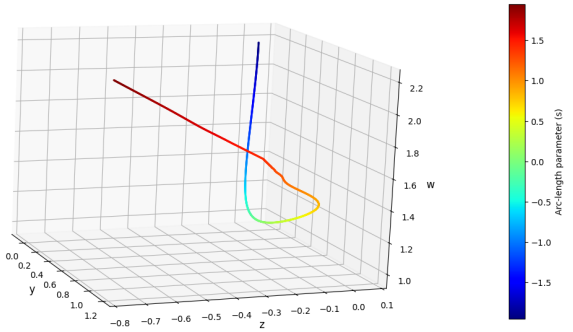

(d) Projection onto yzw space.

Figure 6. Orthogonal projections of the curve $\gamma(s) \subset \mathbb{E}^4$ generated with the deformation parameters $a = b = c = 1$ and $d = \sqrt{2}$. The color indicates the arc-length parameter s. While (a) displays the trajectory in the standard 3D space (xyz), plots (b), (c), and (d) reveal the extension into the fourth dimension (w).

7. Conclusions

The primary objective of this study is to examine the geometric features and attributes of helices in the 4D Euclidean space $\mathbb{E}^4$ using both parallel and Frenet transport frames. The intricacy and richer Frenet apparatus provided by $\mathbb{E}^4$, which permits up to three Frenet curvatures $(\kappa_1, \kappa_2, \kappa_3)$ and allows a more sophisticated categorization of curves than $\mathbb{E}^3$, are considered. To categorize different types of generalized helices, this study effectively developed sufficient and necessary requirements for the curvatures and related vector fields. Specifically, these are as follows.

- The curvature criteria of V_1-helices were described (2.15). In $\mathbb{E}^4$, a curve is a V_1-helix iff it rests on a cylinder and its principal normal vector field maintains a constant angle with the cylinder's normal vector field, according to the geometric interpretation of the definition. Additionally, a

V_1-helix example is provided, and Python is used to observe its projections onto 3D planes (see Figure 2).

- By looking at the relationships between their curvatures and associated vector fields, conditions were determined for V_2-helices (3.12), V_3-helices (4.12), and V_4-helices (5.15).
- For the general case, helices were also described in more generic examples with complex conditions involving curvature functions and several constants (see Eqs (6.12) and (6.13)). The study also provided a requirement that a helix connected to a vector field orthogonal to an axis V and having an F-constant must be contained inside a cylinder (6.14).

Table 1 presents a consolidated summary of the characterization conditions derived for V_i-helices throughout this study.

Table 1. Summary of the necessary and sufficient conditions for V_i-helices in $\mathbb{E}^4$.

Helix type	Axis condition (curvature ratio)	Differential condition
V_1-helix	$C_{3,2} = -\frac{\sin\rho\cos\rho\cos\xi}{\sin^2\rho+\cos^2\rho\sin^2\xi}$	$\frac{\kappa_1^2+\cot\rho\sin\xi(\kappa_3^2\cot\rho\sin\xi+C'_{3,1}\kappa_1)}{\kappa_2\kappa_3\cot\rho\sin\xi+C'_{2,1}\kappa_1} = \tan\xi$
V_2-helix	$C_{2,1} = -\frac{\tan^2\rho+\sin^2\xi}{\cos\xi\sin\xi}$	$\cot\rho\sin\xi\left(\cot\rho\sin\xi C_{3,2}C_{3,1}+\frac{C'_{3,1}}{\kappa_2}\right)+C_{1,2}=\tan\xi$
V_3-helix	$C_{3,2} = \tan\rho\sin\xi$	$C_{1,3}^2 = -\frac{\cot\xi}{\kappa_3}C'_{1,3} - \frac{\cot^2\xi}{\sin^2\rho}$
V_4-helix	$C_{1,2} = -\tan\rho\cos\xi$	$2\left(\sin\xi\frac{C'_{2,3}}{\kappa_3} - C_{2,3}^2\tan\rho\sin^2\xi\right) = \sin 2\rho$

In higher-dimensional Euclidean spaces, the results of this study add to the classical differential geometry of curves. Generalized helices are crucial templates for constructing geometries with specific torsional and curvature characteristics in various domains, including computer-aided geometric design, physics (such as DNA molecules), and robotics (such as trajectory planning). Therefore, they are of great theoretical and practical significance.

In future studies, we aim to extend these characterizations to non-null curves in Lorentzian spaces. Furthermore, given the importance of helical structures in trajectory planning and kinematics, we plan to investigate the potential applications of these high-dimensional helices in robotics and computer-aided geometric design, specifically focusing on the visualization and animation of these curves in dynamic environments.

Author contributions

Derya Sağlam, Umut Selvi, Faik Babadağ, and Ali Atasoy: Conceptualization, Methodology, Validation, Writing-original draft, Writing-review & editing. All authors contributed equally to the conceptualization, methodology, investigation, writing, and editing of the manuscript.

Use of Generative-AI tools declaration

The authors declare they have not used artificial intelligence (AI) tools in the creation of this article.

Conflict of interest

The authors declare that they have no competing financial interests or personal relationships that could influence the work reported in this study.

References

1. A. Mennınger, Characterization of the slant helix as successor curve of the general helix, *Int. Electron. J. Geom.*, **7** (2014), 84–91. https://doi.org/10.36890/iejg.593986
2. A. Şenol, E. Ziplar, Y. Yayli, İ. Gök, A new approach on helices in Euclidean n-space, *Math. Commun.*, **18** (2013), 241–256.
3. A. T. Ali, Position vectors of spacelike general helices in Minkowski 3-space, *Nonlinear Anal.-Theor.*, **73** (2010), 1118–1126. https://doi.org/10.1016/j.na.2010.04.051
4. A. T. Ali, R. López, Some characterizations of inclined curves in Euclidean $\mathbb{E}^n$ space, *Novi Sad J. Math.*, **40** (2010), 9–17.
5. Ç. Camcı, K. İlarslan, L. Kula, H. H. Hacısalihoğlu, Harmonic curvatures and generalized helices in $\mathbb{E}^n$, *Chaos Soliton. Fract.*, **40** (2009), 2590–2596. https://doi.org/10.1016/j.chaos.2007.11.001
6. D. Sağlam, On dual slant helices in $\mathbb{D}^3$, *Adv. Math.*, **11** (2022), 577–589. https://doi.org/10.37418/amsj.11.7.2
7. E. Ziplar, A. Şenol, Y. Yayli, On Darboux helices in Euclidean 3-space, *Global Journal of Science Frontier Research Mathematics and Decision Sciences*, **12** (2012), 73–80.
8. H. A. Hayden, On a generalized helix in a Riemannian n-space, *Proce. Lond. Math. Soc.*, **s2-32** (1931), 337–345. https://doi.org/10.1112/plms/s2-32.1.337
9. İ. Gök, C. Camci, H. Hacısalihoğlu, V_n-slant helices in Euclidean n-space E^n, *Math. Commun.*, **14** (2009), 317–329.
10. M. Barros, General helices and a theorem of Lancret, *Proce. Amer. Math. Soc.*, **125** (1997), 1503–1509.
11. M. Barros, A. Ferrandez, P. Lusas, M. A. Merono, General helices in the three-dimensional Lorentzian space forms, *The Rocky Mountain Journal of Mathematics*, **31** (2001), 373–388.
12. L. Kula, Y. Yaylı, On slant helix and its spherical indicatrix, *Appl. Math. Comput.*, **169** (2005), 600–607. https://doi.org/10.1016/j.amc.2004.09.078
13. P. Lucas, J. A. Ortega-Yagües, Slant helices in the Euclidean 3-space revisited, *Bull. Belg. Math. Soc. Simon Stevin*, **23** (2016), 133–150. https://doi.org/10.36045/bbms/1457560859
14. P. Lucas, J. A. Ortega-Yagües, A generalization of the notion of helix, *Turk. J. Math.*, **47** (2023), 1158–1168. https://doi.org/10.55730/1300-0098.3418
15. U. Öztürk, Z. B. Alkan, Darboux helices in three dimensional Lie groups, *AIMS Mathematics*, **5** (2020), 3169–3181. https://doi.org/10.3934/math.2020204
16. X. Yang, High accuracy approximation of helices by quintic curves, *Comput. Aided Geom. D.*, **20** (2003), 303–317. https://doi.org/10.1016/S0167-8396(03)00074-8

17. Y. Ünlütürk, T. Korpmar, M. Çimdiker, On k-type pseudo null slant helices due to the Bishop frame in Minkowski 3-space $\mathbb{E}_1^3$, *AIMS Mathematics*, **5** (2019), 286–299. https://doi.org/10.3934/math.2020019

18. A. Macdonald, A survey of geometric algebra and geometric calculus, *Adv. Appl. Clifford Algebras*, **27** (2017), 853–891. https://doi.org/10.1007/s00006-016-0665-y

19. E. Özdamar, Characterizations of spherical curves in euclidean n-space, *Commun. Fac. Sci. Univ.*, **23** (1974), 110–125. https://doi.org/10.1501/Commua1_0000000619

20. F. G. Montoya, J. Ventura, F. M. Arrabal-Campos, A. Alcayde, A. H. Eid, Frequency generalization via Darboux bivector and electrical curves in multi-phase power systems, TechRxiv. https://doi.org/10.36227/techrxiv.22829084.v1

21. J. Monterde, Salkowski curves revisited: a family of curves with constant curvature and non-constant torsion, *Comput. Aided Geom. D.*, **26** (2009), 271–278. https://doi.org/10.1016/J.CAGD.2008.10.002

Appendix A. Numerical implementation details of Examples 2.1, 3.1, 4.1, and 5.1

The system of differential equations was solved using the Runge-Kutta-Fehlberg method (RK45) implemented in the `scipy.integrate.solve_ivp` routine.

Initial Conditions: The integration was initialized at an arc-length parameter $s = 0$. The curve was set to start at the origin ($\mathbf{x}(0) = \mathbf{0}$), and the initial Frenet frame vectors $\{V_1, V_2, V_3, V_4\}$ were aligned with the standard orthonormal basis of $\mathbb{E}^4$. Accordingly, the initial state vector Y_0 is defined as

$$Y_0 = \Big[\underbrace{0,0,0,0}_{\text{Position}},\underbrace{1,0,0,0}_{V_1},\underbrace{0,1,0,0}_{V_2},\underbrace{0,0,1,0}_{V_3},\underbrace{0,0,0,1}_{V_4}\Big]^T.$$

Tolerances: The relative tolerance (`rtol`) was set to 10^{-9} and the absolute tolerance (`atol`) to 10^{-10}. These strict tolerance levels were selected to ensure that the local truncation errors remained orders of magnitude smaller than the characteristic scales of the dynamic variables. To verify the sufficiency, convergence tests were performed by tightening the tolerances to 10^{-12}, which yielded no numerically significant deviations from the reported trajectories.

Appendix 1.

```
import numpy as np
import matplotlib.pyplot as plt
from scipy.integrate import solve_ivp
from mpl_toolkits.mplot3d import Axes3D

def plot_individual_projections():
# --- 1. Parameters ---
c = 1.0
s_limit = 3.10 / c
s_span = [-s_limit, s_limit]
s_eval = np.linspace(-s_limit, s_limit, 10000)

# --- 2. 4D Frenet Solver (Same logic as before) ---
def frenet_4d_system(s, Y):
```

```
        V1, V2, V3, V4 = Y[4:8], Y[8:12], Y[12:16], Y[16:20]

        # Curvatures
        k1 = c
        k2 = (3 * c / 2) * np.tan(c * s / 2)
        k3 = -(np.sqrt(2) * c / 2) * np.tan(c * s / 2)

        # Derivatives
        dPos = V1
        dV1  = k1 * V2
        dV2  = -k1 * V1 + k2 * V3
        dV3  = -k2 * V2 + k3 * V4
        dV4  = -k3 * V3

        return np.concatenate([dPos, dV1, dV2, dV3, dV4])

    # Initial Conditions
    Y0 = np.zeros(20)
    Y0[4:8]   = [1, 0, 0, 0] # V1
    Y0[8:12]  = [0, 1, 0, 0] # V2
    Y0[12:16] = [0, 0, 1, 0] # V3
    Y0[16:20] = [0, 0, 0, 1] # V4

    # Solve
    print("Solving differential equations...")
    sol = solve_ivp(frenet_4d_system, s_span, Y0, t_eval=s_eval,
                    method='RK45', rtol=1e-9, atol=1e-10)

    x, y, z, w = sol.y[0:4]
    colors = s_eval # Color by arc-length

    # --- 3. Plotting Individual Figures ---

    # Helper function to create consistent plots
    def create_single_plot(x_data, y_data, z_data,
                           x_label, y_label, z_label,
                           title, filename):
        fig = plt.figure(figsize=(10, 8))
        ax = fig.add_subplot(111, projection='3d')
        sc = ax.scatter(x_data, y_data, z_data, c=colors, cmap='jet', s=1)

        ax.set_xlabel(x_label, fontsize=12)
        ax.set_ylabel(y_label, fontsize=12)
        ax.set_zlabel(z_label, fontsize=12)
        ax.set_title(title, fontsize=14)
        ax.view_init(elev=30, azim=-45)

        # Colorbar
        cbar = plt.colorbar(sc, pad=0.1, shrink=0.7)
        cbar.set_label('Arc-length parameter (s)')

        plt.tight_layout()
        # Uncomment the line below to save the figure automatically
        # plt.savefig(filename, dpi=300)
        print(f"Generated: {title}")
        plt.show()

    # --- Figure 1: XYZ Projection ---
    create_single_plot(x, y, z,
```

```
                      "x", "y", "z",
                      "",
                      "figure_xyz.png")

    # --- Figure 2: XYW Projection ---
    create_single_plot(x, y, w,
                      "x", "y", "w",
                      "",
                      "figure_xyw.png")

    # --- Figure 3: XZW Projection ---
    create_single_plot(x, z, w,
                      "x", "z", "w",
                      "",
                      "figure_xzw.png")

    # --- Figure 4: YZW Projection (The Helical Structure) ---
    # Changing view angle for this specific one to match previous best view
    fig = plt.figure(figsize=(10, 8))
    ax = fig.add_subplot(111, projection='3d')
    sc = ax.scatter(y, z, w, c=colors, cmap='jet', s=1)
    ax.set_xlabel("y", fontsize=12)
    ax.set_ylabel("z", fontsize=12)
    ax.set_zlabel("w", fontsize=12)
    ax.set_title("", fontsize=14)
    ax.view_init(elev=30, azim=45) # Different angle for better view
    plt.colorbar(sc, pad=0.1, shrink=0.7).set_label('Arc-length parameter (s)')
    plt.tight_layout()
    # plt.savefig("figure_yzw.png", dpi=300)
    print("Generated: Projection onto YZW Subspace")
    plt.show()

    if __name__ == "__main__":
    plot_individual_projections()
```

Listing 1. Python script for solving the 4D Frenet system and plotting projections.

Appendix 2.

```
    import numpy as np
    import matplotlib.pyplot as plt
    from scipy.integrate import solve_ivp
    from mpl_toolkits.mplot3d import Axes3D

    def plot_individual_projections():
    # --- 1. Parameters ---
    c = 1.0
    s_limit = 0.89 / c
    s_span = [-s_limit, s_limit]
    s_eval = np.linspace(-s_limit, s_limit, 3000)

    # --- 2. 4D Frenet Solver (Same logic as before) ---
    def frenet_4d_system(s, Y):
        V1, V2, V3, V4 = Y[4:8], Y[8:12], Y[12:16], Y[16:20]

        # Curvatures
        k1 = 1.0
        k2 = 2.0
        k3 = np.sqrt(3) * np.tan(np.sqrt(3) * s)

```

```
        # Derivatives
        dPos = V1
        dV1   = k1 * V2
        dV2   = -k1 * V1 + k2 * V3
        dV3  = -k2 * V2 + k3 * V4
        dV4  = -k3 * V3

        return np.concatenate([dPos, dV1, dV2, dV3, dV4])

    # Initial Conditions
    Y0 = np.zeros(20)
    Y0[4:8]   = [1, 0, 0, 0] # V1
    Y0[8:12]  = [0, 1, 0, 0] # V2
    Y0[12:16] = [0, 0, 1, 0] # V3
    Y0[16:20] = [0, 0, 0, 1] # V4

    # Solve
    print("Solving differential equations...")
    sol = solve_ivp(frenet_4d_system, s_span, Y0, t_eval=s_eval,
                    method='RK45', rtol=1e-9, atol=1e-10)

    x, y, z, w = sol.y[0:4]
    colors = s_eval # Color by arc-length

    # --- 3. Plotting Individual Figures ---

    # Helper function to create consistent plots
    def create_single_plot(x_data, y_data, z_data,
                           x_label, y_label, z_label,
                           title, filename):
        fig = plt.figure(figsize=(10, 8))
        ax = fig.add_subplot(111, projection='3d')
        sc = ax.scatter(x_data, y_data, z_data, c=colors, cmap='jet', s=1)

        ax.set_xlabel(x_label, fontsize=12)
        ax.set_ylabel(y_label, fontsize=12)
        ax.set_zlabel(z_label, fontsize=12)
        ax.set_title(title, fontsize=14)
        ax.view_init(elev=30, azim=-45)

        # Colorbar
        cbar = plt.colorbar(sc, pad=0.1, shrink=0.7)
        cbar.set_label('Arc-length parameter (s)')

        plt.tight_layout()
        # Uncomment the line below to save the figure automatically
        # plt.savefig(filename, dpi=300)
        print(f"Generated: {title}")
        plt.show()

    # --- Figure 1: XYZ Projection ---
    create_single_plot(x, y, z,
                       "x", "y", "z",
                       "",
                       "figure_xyz.png")

    # --- Figure 2: XYW Projection ---
    create_single_plot(x, y, w,
                       "x", "y", "w",
```

```
                        "",
                        "figure_xyw.png")

    # --- Figure 3: XZW Projection ---
    create_single_plot(x, z, w,
                        "x", "z", "w",
                        "",
                        "figure_xzw.png")

    # --- Figure 4: YZW Projection (The Helical Structure) ---
    # Changing view angle for this specific one to match previous best view
    fig = plt.figure(figsize=(10, 8))
    ax = fig.add_subplot(111, projection='3d')
    sc = ax.scatter(y, z, w, c=colors, cmap='jet', s=1)
    ax.set_xlabel("y", fontsize=12)
    ax.set_ylabel("z", fontsize=12)
    ax.set_zlabel("w", fontsize=12)
    ax.set_title("", fontsize=14)
    ax.view_init(elev=30, azim=45) # Different angle for better view
    plt.colorbar(sc, pad=0.1, shrink=0.7).set_label('Arc-length parameter (s)')
    plt.tight_layout()
    # plt.savefig("figure_yzw.png", dpi=300)
    print("Generated: Projection onto YZW Subspace")
    plt.show()

    if __name__ == "__main__":
    plot_individual_projections()
```

Listing 2. Python script for solving the 4D Frenet system and plotting projections.

Appendix 3.

```
    import numpy as np
    import matplotlib.pyplot as plt
    from scipy.integrate import solve_ivp
    from mpl_toolkits.mplot3d import Axes3D

    def plot_individual_projections():
    # --- 1. Parameters ---
    c = 1.0
    s_limit = 100 / c
    s_span = [-s_limit, s_limit]
    s_eval = np.linspace(-s_limit, s_limit, 10000)

    # --- 2. 4D Frenet Solver (Same logic as before) ---
    def frenet_4d_system(s, Y):
        V1, V2, V3, V4 = Y[4:8], Y[8:12], Y[12:16], Y[16:20]

        # Curvatures
        k1 = -s / (s**2 + 2)
        k2 = -np.sqrt(2) / (s**2 + 2)
        k3 = -1 / (s**2 + 2)

        # Derivatives
        dPos = V1
        dV1  = k1 * V2
        dV2  = -k1 * V1 + k2 * V3
        dV3  = -k2 * V2 + k3 * V4
        dV4  = -k3 * V3

```

```
        return np.concatenate([dPos, dV1, dV2, dV3, dV4])

    # Initial Conditions
    Y0 = np.zeros(20)
    Y0[4:8]   = [1, 0, 0, 0] # V1
    Y0[8:12]  = [0, 1, 0, 0] # V2
    Y0[12:16] = [0, 0, 1, 0] # V3
    Y0[16:20] = [0, 0, 0, 1] # V4

    # Solve
    print("Solving differential equations...")
    sol = solve_ivp(frenet_4d_system, s_span, Y0, t_eval=s_eval,
                    method='RK45', rtol=1e-9, atol=1e-10)

    x, y, z, w = sol.y[0:4]
    colors = s_eval # Color by arc-length

    # --- 3. Plotting Individual Figures ---

    # Helper function to create consistent plots
    def create_single_plot(x_data, y_data, z_data,
                           x_label, y_label, z_label,
                           title, filename):
        fig = plt.figure(figsize=(10, 8))
        ax = fig.add_subplot(111, projection='3d')
        sc = ax.scatter(x_data, y_data, z_data, c=colors, cmap='jet', s=1)

        ax.set_xlabel(x_label, fontsize=12)
        ax.set_ylabel(y_label, fontsize=12)
        ax.set_zlabel(z_label, fontsize=12)
        ax.set_title(title, fontsize=14)
        ax.view_init(elev=30, azim=-45)

        # Colorbar
        cbar = plt.colorbar(sc, pad=0.1, shrink=0.7)
        cbar.set_label('Arc-length parameter (s)')

        plt.tight_layout()
        # Uncomment the line below to save the figure automatically
        # plt.savefig(filename, dpi=300)
        print(f"Generated: {title}")
        plt.show()

    # --- Figure 1: XYZ Projection ---
    create_single_plot(x, y, z,
                       "x", "y", "z",
                       "",
                       "figure_xyz.png")

    # --- Figure 2: XYW Projection ---
    create_single_plot(x, y, w,
                       "x", "y", "w",
                       "",
                       "figure_xyw.png")

    # --- Figure 3: XZW Projection ---
    create_single_plot(x, z, w,
                       "x", "z", "w",
                       "",
```

```
                        "figure_xzw.png")

    # --- Figure 4: YZW Projection (The Helical Structure) ---
    # Changing view angle for this specific one to match previous best view
    fig = plt.figure(figsize=(10, 8))
    ax = fig.add_subplot(111, projection='3d')
    sc = ax.scatter(y, z, w, c=colors, cmap='jet', s=1)
    ax.set_xlabel("y", fontsize=12)
    ax.set_ylabel("z", fontsize=12)
    ax.set_zlabel("w", fontsize=12)
    ax.set_title("", fontsize=14)
    ax.view_init(elev=30, azim=45) # Different angle for better view
    plt.colorbar(sc, pad=0.1, shrink=0.7).set_label('Arc-length parameter (s)')
    plt.tight_layout()
    # plt.savefig("figure_yzw.png", dpi=300)
    print("Generated: Projection onto YZW Subspace")
    plt.show()

    if __name__ == "__main__":
    plot_individual_projections()
```

Listing 3. Python script for solving the 4D Frenet system and plotting projections.

Appendix 4.

```
import numpy as np
import matplotlib.pyplot as plt
from scipy.integrate import solve_ivp
from mpl_toolkits.mplot3d import Axes3D

def plot_individual_projections():
# --- 1. Parameters ---
c = 1.0
s_limit = 50 / c
s_span = [-s_limit, s_limit]
s_eval = np.linspace(-s_limit, s_limit, 10000)

# --- 2. 4D Frenet Solver (Same logic as before) ---
def frenet_4d_system(s, Y):
    V1, V2, V3, V4 = Y[4:8], Y[8:12], Y[12:16], Y[16:20]

    # Curvatures
    k1 = -s /(1 + s**2)
    k2 = (s * np.sqrt(2)) / (1 + s**2)
    k3 = np.sqrt(2) / (1 + s**2)

    # Derivatives
    dPos = V1
    dV1  = k1 * V2
    dV2  = -k1 * V1 + k2 * V3
    dV3  = -k2 * V2 + k3 * V4
    dV4  = -k3 * V3

    return np.concatenate([dPos, dV1, dV2, dV3, dV4])

# Initial Conditions
Y0 = np.zeros(20)
Y0[4:8]   = [1, 0, 0, 0] # V1
Y0[8:12]  = [0, 1, 0, 0] # V2
Y0[12:16] = [0, 0, 1, 0] # V3
```

```
    Y0[16:20] = [0, 0, 0, 1] # V4

    # Solve
    print("Solving differential equations...")
    sol = solve_ivp(frenet_4d_system, s_span, Y0, t_eval=s_eval,
                    method='RK45', rtol=1e-9, atol=1e-10)

    x, y, z, w = sol.y[0:4]
    colors = s_eval # Color by arc-length

    # --- 3. Plotting Individual Figures ---

    # Helper function to create consistent plots
    def create_single_plot(x_data, y_data, z_data,
                           x_label, y_label, z_label,
                           title, filename):
        fig = plt.figure(figsize=(10, 8))
        ax = fig.add_subplot(111, projection='3d')
        sc = ax.scatter(x_data, y_data, z_data, c=colors, cmap='jet', s=1)

        ax.set_xlabel(x_label, fontsize=12)
        ax.set_ylabel(y_label, fontsize=12)
        ax.set_zlabel(z_label, fontsize=12)
        ax.set_title(title, fontsize=14)
        ax.view_init(elev=30, azim=-45)

        # Colorbar
        cbar = plt.colorbar(sc, pad=0.1, shrink=0.7)
        cbar.set_label('Arc-length parameter (s)')

        plt.tight_layout()
        # Uncomment the line below to save the figure automatically
        # plt.savefig(filename, dpi=300)
        print(f"Generated: {title}")
        plt.show()

    # --- Figure 1: XYZ Projection ---
    create_single_plot(x, y, z,
                       "x", "y", "z",
                       "",
                       "figure_xyz.png")

    # --- Figure 2: XYW Projection ---
    create_single_plot(x, y, w,
                       "x", "y", "w",
                       "",
                       "figure_xyw.png")

    # --- Figure 3: XZW Projection ---
    create_single_plot(x, z, w,
                       "x", "z", "w",
                       "",
                       "figure_xzw.png")

    # --- Figure 4: YZW Projection (The Helical Structure) ---
    # Changing view angle for this specific one to match previous best view
    fig = plt.figure(figsize=(10, 8))
    ax = fig.add_subplot(111, projection='3d')
    sc = ax.scatter(y, z, w, c=colors, cmap='jet', s=1)
```

```
    ax.set_xlabel("y", fontsize=12)
    ax.set_ylabel("z", fontsize=12)
    ax.set_zlabel("w", fontsize=12)
    ax.set_title("", fontsize=14)
    ax.view_init(elev=30, azim=45) # Different angle for better view
    plt.colorbar(sc, pad=0.1, shrink=0.7).set_label('Arc-length parameter (s)')
    plt.tight_layout()
    # plt.savefig("figure_yzw.png", dpi=300)
    print("Generated: Projection onto YZW Subspace")
    plt.show()

    if __name__ == "__main__":
    plot_individual_projections()
```

Listing 4. Python script for solving the 4D Frenet system and plotting projections.

Appendix B. Numerical implementation details of Example 6.1

The algorithm reconstructs the curve $\gamma(s)$ in $\mathbb{E}^4$ by integrating the Frenet-Serret system. The numerical scheme operates on the basis of the following principles.

Integration Method: The differential equations are solved using the *explicit Euler method* with a step size determined by the discretization of the interval $[-1.95, 1.95]$ into 4000 points.

Stability: To prevent the numerical drift inherent to first-order integration, a normalization step ($\|V_i\| = 1$) is applied at each iteration to maintain the orthonormality of the frame.

Fourth Dimension: The coordinate $w(s)$ is computed analytically as $w = \sqrt{1 + s^2}$ alongside the numerical integration of the spatial components.

Initial Conditions: The simulation was initialized with the position vector set to the origin, $\alpha = (0, 0, 0)$. The initial Frenet frame vectors $\{V_1, V_2, V_3\}$ were aligned with the standard orthonormal basis of $\mathbb{E}^3$ as follows:

$$V_1 = (1, 0, 0), \quad V_2 = (0, 1, 0), \quad V_3 = (0, 0, 1).$$

These conditions serve as the starting point for the iterative update loop presented in Appendix 5.

Appendix 5.

```
import numpy as np
import matplotlib.pyplot as plt
from mpl_toolkits.mplot3d import Axes3D

print("Calculating projections...")

# --- 1. Parameters ---
limit = 1.95
s_vals = np.linspace(-limit, limit, 4000)
ds = s_vals[1] - s_vals[0]

# --- 2. Initial Conditions ---
alpha = np.array([0.0, 0.0, 0.0]) # Represents x, y, z
V1 = np.array([1.0, 0.0, 0.0])
V2 = np.array([0.0, 1.0, 0.0])
V3 = np.array([0.0, 0.0, 1.0])

x_list, y_list, z_list, w_list = [], [], [], []

```

```
    # --- 3. Calculation (Euler Integration) ---
    for s in s_vals:
        x_list.append(alpha[0])
        y_list.append(alpha[1])
        z_list.append(alpha[2])
        w_list.append(np.sqrt(1 + s**2)) # w (The 4th dimension)

        # Curvature and Torsion parameters
        rho = np.pi/4 + np.arcsin(s/2.0)
        cos_rho = np.cos(rho)
        if abs(cos_rho) < 1e-6: cos_rho = 1e-6 * np.sign(cos_rho)

        kappa = np.tan(rho)
        u_prime = s / np.sqrt(1 + s**2)
        tau = -(1.0/cos_rho) * kappa * u_prime

        # Frenet Update
        new_V1 = V1 + (kappa * V2) * ds
        new_V2 = V2 + (-kappa * V1 + tau * V3) * ds
        new_V3 = V3 + (-tau * V2) * ds

        alpha = alpha + V1 * ds

        # Normalization for stability
        V1 = new_V1 / np.linalg.norm(new_V1)
        V2 = new_V2 / np.linalg.norm(new_V2)
        V3 = new_V3 / np.linalg.norm(new_V3)

    # --- 4. Plotting Individual Figures ---

    def create_clean_plot(data_a, data_b, data_c, labels):
        fig = plt.figure(figsize=(10, 8))
        ax = fig.add_subplot(111, projection='3d')

        # Scatter plot with color mapping (jet colormap)
        sc = ax.scatter(data_a, data_b, data_c, c=s_vals, cmap='jet', s=1.5)

        # Axis labels: x, y, z, w
        ax.set_xlabel(labels[0], fontsize=12)
        ax.set_ylabel(labels[1], fontsize=12)
        ax.set_zlabel(labels[2], fontsize=12)

        # Colorbar configuration
        cbar = plt.colorbar(sc, pad=0.1, shrink=0.7)
        cbar.set_label('Arc-length parameter (s)')

        # View angle for better 3D perception
        ax.view_init(elev=30, azim=-45)

        plt.tight_layout()
        plt.show()

    # --- Figure 1: XYZ Projection ---
    print("Displaying: Projection x, y, z")
    create_clean_plot(x_list, y_list, z_list, ["x", "y", "z"])

    # --- Figure 2: XYW Projection ---
    print("Displaying: Projection x, y, w")
    create_clean_plot(x_list, y_list, w_list, ["x", "y", "w"])
```

```
79
80      # --- Figure 3: XZW Projection ---
81      print("Displaying: Projection x, z, w")
82      create_clean_plot(x_list, z_list, w_list, ["x", "z", "w"])
83
84      # --- Figure 4: YZW Projection ---
85      print("Displaying: Projection y, z, w")
86      create_clean_plot(y_list, z_list, w_list, ["y", "z", "w"])
```

Listing 5. Python script for solving the 4D Frenet system and plotting projections.

AIMS Press